Nanofabrication and its application in developing high aspect ratio (HAR) and edge Atomic Force Microscopy (AFM) probes

by

Chenxu Zhu

A thesis

Presented to University of Waterloo

in the fulfillment of the

thesis requirement for the degree of

Master of Applied Science

in

Electrical and Computer Engineering (Nanotechnology)

Waterloo, Ontario, Canada, 2018

Author’s Declaration

I hereby declare that I am the sole author of this thesis. This is a true copy of the thesis, including any required final revisions, as accepted by my examiners.

I understand that my thesis may be made electronically available to the public.

Abstract

This thesis focuses on nanofabrication and its applications which are related to producing atomic force microscope (AFM) probes.

This thesis is divided into four chapters. The first chapter brings a preliminary introduction to nanofabrication. The second chapter reviews the history of AFM and fabrication process of AFM probe. Equipping with the basic knowledge, Chapter 3, the main chapter, goes to our work on the batch fabrication of high aspect ratio (HAR) AFM tips. Last but not least, Chapter 4 focuses on another work, batch fabrication of edge probes. In order to obtain a more accurate image of surfaces, high aspect ratio tips are needed to reach the bottom of very deep and narrow trenches. However, currently all commercial HAR tips are produced in a slow, high-cost (~5-20× that of regular AFM tips) way. We have developed a new method to batch fabricate HAR tips. In this fabrication, two kinds of hard masks were deposited at a specific angle followed by two etching processes (dry etching and wet etching respectively). As a result, a small piece of hard mask was formed just on the apex of pyramid tip, which would be the protection layer in the following RIE step. The batch and lithography-free process makes it an efficient and low-cost method. The controllable profile, radius of curvature and aspect ratio of tips can be easily obtained by adjusting gas ratio and etching time in RIE. All the parameters and results were demonstrated clearly assisted by images and schematics. For edge probes, our method to batch fabricate tips on the edge is introduced step by step as well. The objective of every step is presented in detail assisted with schematics and tables.

Acknowledgement

This work was carried out by using facilities at Quantum NanoFab, WATLab and Giga-to-Nanoelectronics (G2N) Laboratory in University of Waterloo. Quantum NanoFab infrastructure would not be possible without the significant contributions of the Canada Foundation for Innovation, the Ontario Ministry of Research & Innovation, Industry Canada and Mike & Ophelia Lazaridis. And, G2N laboratory is funded by Canada Foundation for Innovation, the Ontario Ministry of Research & Innovation and Industry Canada. Their supports are always grateful.

Firstly, I would like to sincerely thank my parents for their encouragement and support during my study and research.

I will be glad to acknowledgement my supervisor Prof. Bo Cui. I will not finish this work without his patient guidance and precious suggestions.

Finally, my thanks goes to my group mates Shuo Zheng, Ripon Dey, Ruifeng Yang, Yaoze Liu, and Hang Zhang,

Table of Contents

List of Figures

List of Tables

Chapter 1. Introduction

This chapter provides a brief overview of nanofabrication.

1.1 "Nano" and nanotechnology

The prefix "nano", which is based on the Greek word for dwarf, became part of scientific nomenclature in 1960.[1] This prefix has a factor of 10^{-9} and is frequently encountered in science and technology nowadays.

Nanotechnology is the manipulation of matters and devices in atomic, molecular and supramolecular scale. A more accurate description was established by National Nanotechnology Initiative (NNI), which defines nanotechnology as the technology enabling design and manipulation of matter and device sized from 1 to 100 nanometers (nm) in at least one dimension. Nowadays, nanotechnology is a hot topic, which expands in many fields such as semiconductor physics, computer science, organic chemistry and medicine etc.[2] Fig 1.1 compares nano-scale (1-100 nm) matters with other common materials in our daily life. In the future, nanotechnology may be able to create and produce lots of new materials and devices in the field of technology, engineering etc.

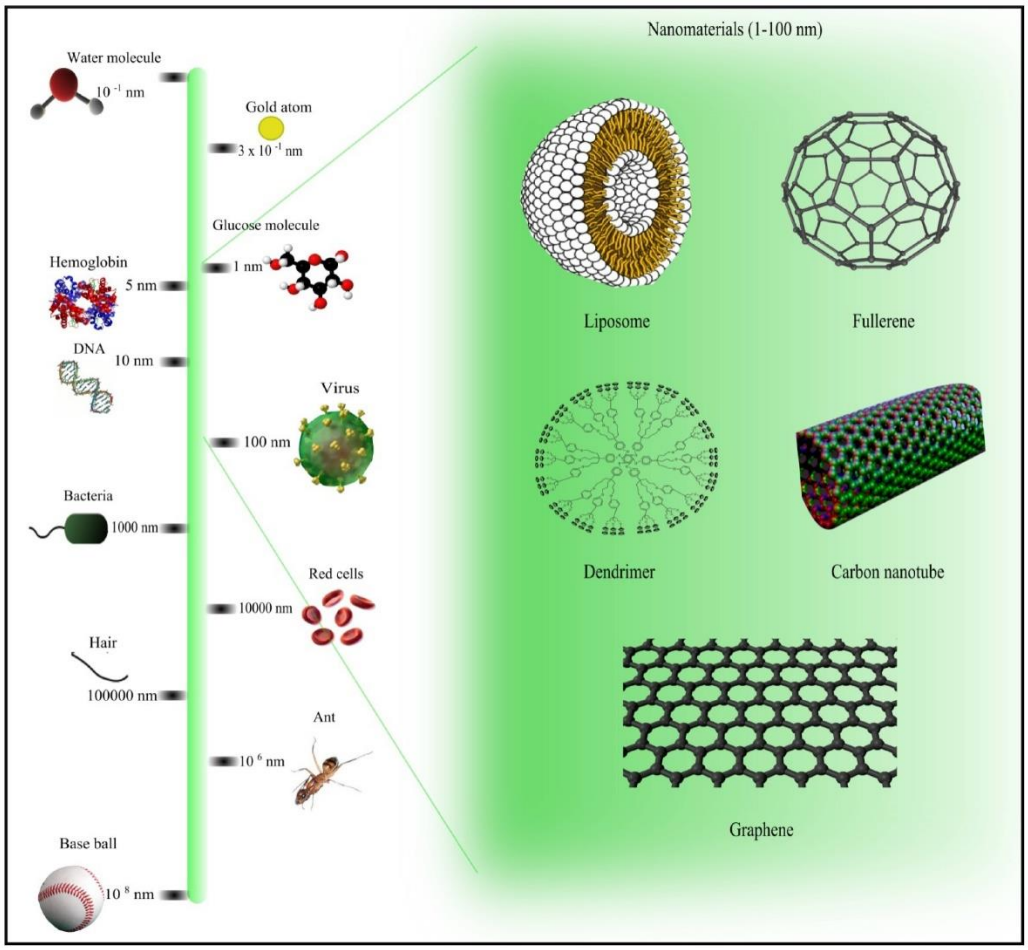

Figure 2.1 Comparison of the sizes of nanomaterials with those of other common materials[3]

1.2 Overview of nanofabrication

Nanofabrication is the process to develop and achieve desired structures in the nanoscale (1-100 nm). In the past ten years, nanofabrication research contributed a lot to the great improvement of nanoelectronic devices and information technologies, which will continue improving the field in future.[4] There are three basic parts of nanofabrication: lithography, thin film deposition, and etching. To achieve all the design and patterning, these three steps are broadly used in two branches of nanofabrication approaches: “Top-down” and “Bottom-up” process.

Bottom-up approach is based on self-assembly fabrication process. It arranges atom, molecular or nanoscale blocks into more complex and ordered assemblies.[5] Fig 1.2b indicates a common bottom-up approach where a patterned monolayer is formed by self-assembly followed by pattern-transfer

from polymer sphere to the substrate. Driven by chemical reaction and phase separation, an ordered pattern can be constructed automatically by self-assembly. There are three most important techniques of self-assembly: block co-polymer self-assembly, porous anodized aluminum oxide, and nano-sphere lithography. The most dramatical advantage is its low cost and saving of materials. However, it also comes with some drawbacks. As a result of self-assembly process, people can only obtain periodic structures, usually without long-range ordering. To figure out what pattern we achieve reproducibly is still a challenging part and requires more research in the future.

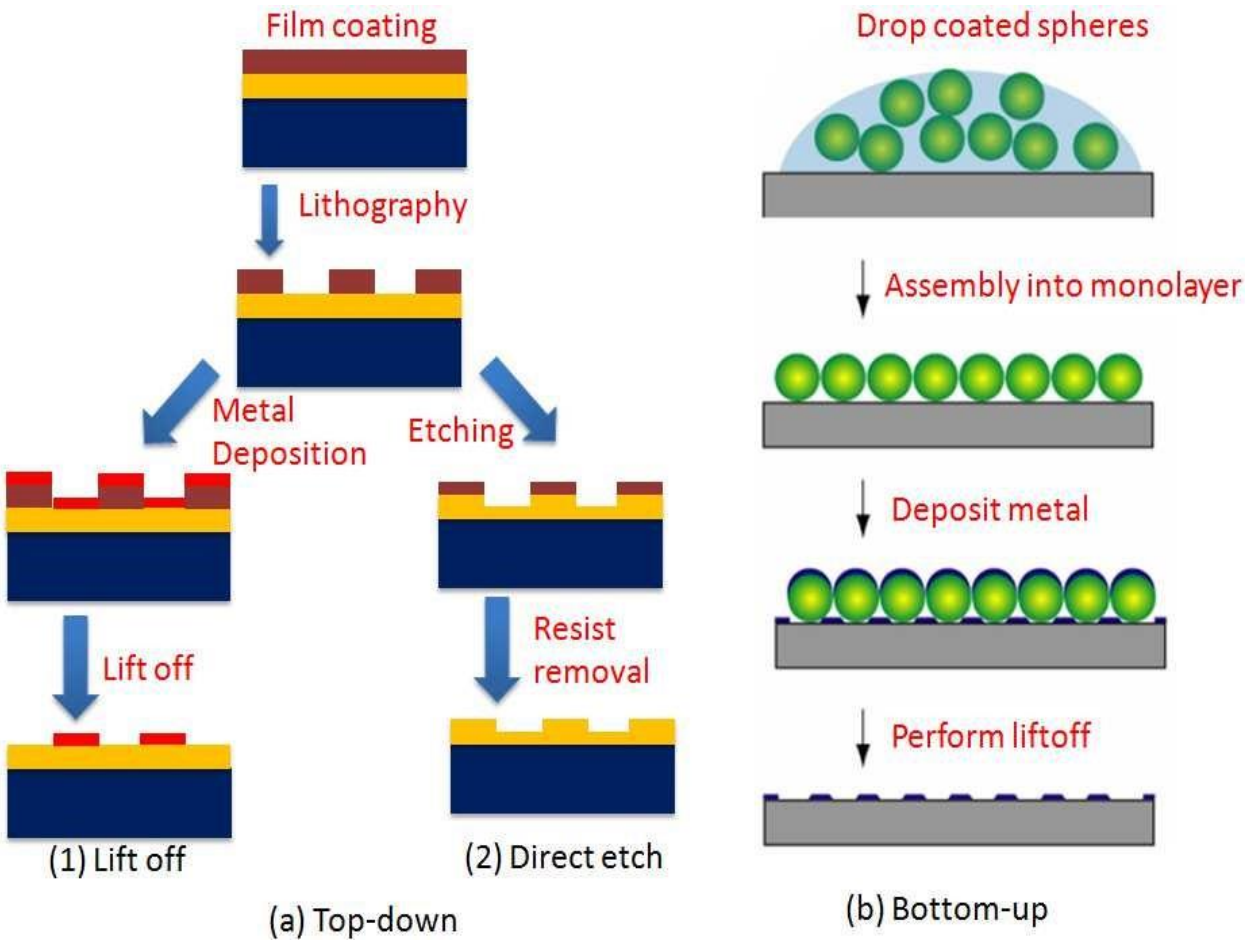

Figure 1.2 The schematic of the (a) top-down and the (b) bottom-up approach. Usually the pattern is created by thin film deposition and lithography in top-down process. Then there are two ways to transfer the pattern to the substrate: lift off or direct etch. In bottom-up approach, the pattern is formed by self-assembly process and transferred by lift off.

On the contrary, top-down approach starts from a large dimension and seeks to reduce it to a desired smaller scale. It includes lithography, thin film deposition, and etching. The lateral structure is defined

mainly by lithography techniques and the vertical feature is executed by thin film deposition and etching.

Since photolithography was first introduced into the integrated circuits (IC) industry in 1960's,[4] various types of lithography techniques have been widely implemented in the top-down process, constructing whatever we want in nanoscale. In general, lithography techniques can be divided into two groups. The first group includes photolithography (or optical lithography), x-ray lithography (XRL), deep ultra-violet lithography (DUVL), extreme ultraviolet lithography (EUVL) and nanoimprint lithography (NIL), and they all duplicate and transfer the pattern from the mask. This method has a high yield and throughput because a large number of copies of the pattern can be created in one run with a high speed; therefore, this is the most ideal method for large-scale commercial production. Currently, the main concern of this kind of lithography is the resolution, which is limited by light diffraction. Typical photolithography can only achieve a resolution of around 1 μm. In order to improve the resolution, several resolution enhancement techniques (RET) have been developed such as off-axis illumination (OAI), phase shift masks (PSM), optical proximity correction (OPC), and double processing, which lead to the resolution down to sub-10 nm. The second group contains electron beam lithography (EBL), ion beam lithography (IBL) and scanning probe lithography (SPL),[6] which construct structures on the resist layer one by one without mask and copy. They can be called "direct patterning lithography" because they draw the pattern directly into the resist layer. Electron beam lithography and ion beam lithography modify the resist by an exposure of electron or ion. Scanning probe lithography (developed from the atomic force microscope invented in 1986[7]) is also a good method to create a pattern by local heating, oxidation and object manipulation. Scanning probe lithography has the highest resolution (one atom) among all the methods. These direct patterning lithography methods attract many people because of their simplicity, straightforward steps, and high resolution. However, as a result of patterning one by one, the throughput of these methods is very hard to increase, hence they are more suitable for research and mask production.

Thin film deposition plays a fundamental role as the addictive process in the top-down approach. A thin film is a layer ranging from few nanometers to few micrometers, which can be attached to the

substrate or previous layer by two main methods: chemical deposition and physical deposition.[8] Chemical deposition means different chemicals called precursors will undergo chemical reactions on the surface and remain as a solid layer. Chemical deposition is categorized by the phase of precursor. It includes electroplating and chemical solution deposition (CSD), which depend on liquid precursors; and chemical vapor deposition (CVD), plasma enhanced CVD (PECVD) and atomic layer deposition (ALD), which use gas precursors. On the contrary, physical vapor deposition uses mechanical or thermodynamic means to release materials from sources and leave a solid layer on the substrate without any chemical reaction. There are two main types of physical deposition: sputter and evaporation. Evaporation process can be found in detail in the next chapter.

Another basic part of top-down approach is etching, which behaves as a subtractive process. It has three steps: transportation of reactants, reactions between reactants and target layer and transportation of reaction products. Depending on the phase of reactants, it is divided into two types: wet etching and dry etching.[9] Wet etching uses liquid etchant to remove materials. It is simple and cheap but may not reproducible. Hence it is not suitable for nanopattern transfer. For dry etching, gas reactants are involved to etch undesired materials. Both methods are going to be introduced in the next chapter and dry etching is used to produce high aspect ratio tip in Chapter 3.

Chapter 2 Introduction to Atomic Force Microscope and tip Fabrication

This chapter provides a detailed introduction of AFM technique, probe fabrication, and particularly high aspect ratio tips.

2.1 Background

2.1.1 History of AFM

Atomic force microscope (AFM) and scanning tunneling microscopy (STM) are both under the family of scanning probe microscopy (SPM). Both mainly "feel" the surface to gather the information of surface. STM was first invented by Binning et al. in 1982[1], making a breakthrough in investigating atomic level surfaces. Followed by the invention of STM principle, STM instrument became more and more popular and right after one year, it helped the scientific community to solve the most intriguing problems in surface science. For instance, the structure of Si (111)-(7x7) surface was characterized by using STM (Binnig et al. in 1983[2]).

Despite having a lot of successes using STM technique, it brought several limitations in applying this technique to the sample. The biggest problem is that the conductivity of the sample is essential. Since STM measure the tunneling current between the tip and sample surface, insulator cannot be characterized by using STM.

With this drawback of STM, scientific community was looking for a new technique to investigate sample surfaces. Later on, Binnig et al. first proposed the atomic force microscope principle in 1986[1]. In principle,

AFM works by measuring short-range force (Van der Waals, hydrogen-bonding, contact) and long-range force (electrostatic force, magneto-electrostatic forces) instead of the tunneling current and does not require conductive sample. The principles of AFM and STM are quite similar (see Fig 2.1, adapted from Binnig et al.,1986). The tip moves and follows contour B of the sample surface. In a case of STM, it measures the tunneling current and keeps it a constant. On the other hand, in AFM technique, the interaction force between tip and sample is measured and maintained to a constant.

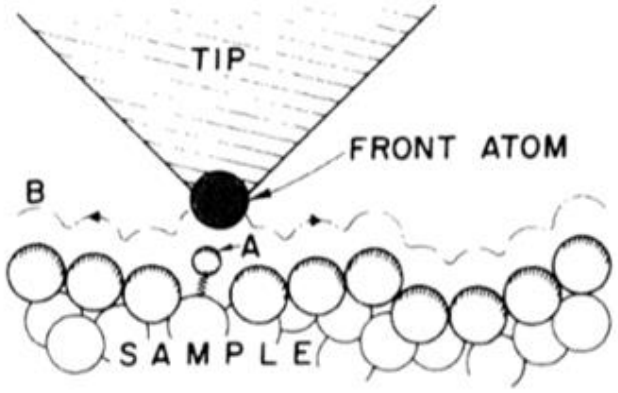

Figure 2.1[1] Description of the principle of the SPM. Tip follows contour B to maintain constant current (STM) and constant force (AFM) between tip and sample.

2.1.2 Principle of operation

The process of AFM operation is shown in Fig 2.2. It begins in gradually narrowing the gap between tip and sample surface until a specific interaction (force) is achieved. When the tip "touch and feel" the sample, the interaction directly causes the deflection of the cantilever arm in AFM probe. In general, sample surface can be scanned and imaged in two ways. One is to maintain the distance between tip and sample unchanged. When scanning different areas, different structures result in deflection changes. This change will be monitored by a feedback system, including laser and an optical sensor. The piezo scanner is able to localize the tip both along the z-axis and x, y-axis. After scanning and recording, the sample topography is finally imaged by digitizing the deflection change. On the contrary, the other way to achieve the same

goal is to keep the deflection constant and measure the distance change. The interaction between tip and sample is controlled by the feedback controller in z-axis, which also tells the piezo scanner how much in z-axis it should be moved to maintain the same deflection. This is very straightforward since the amount of movement in z-axis equals to the height of the sample. AFM is able to provide an atomic resolution, and unlike another popular imaging machine: scanning electron microscope (SEM), which needs vacuum environment, AFM can work under air or liquid.

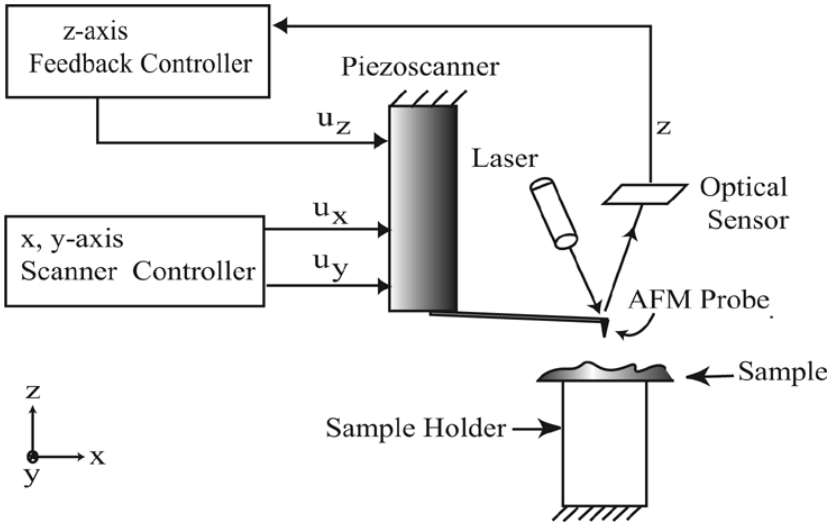

Figure 2.2[3] Schematic diagram of AFM operation.

2.1.3 Imaging mode

Typically, there are three basic imagining modes of AFM: static mode (which is also called contact mode) and its counterpart dynamic mode (including non-contact mode and tapping mode).

2.1.3.1 Contact mode

Just as the name implies, in contact mode, the tip contacts the sample surface and is dragged to scan the contour. In this mode, atoms experience repulsive force, which is sensitive to distance because of the contacting. As a result, this mode achieves high resolution easily.

However, a big challenge of contact mode is tip-induced irreversible damage. For instance, the silica surface with a UV curable urethane-acrylate residual polymer cannot be image accurately under contact mode since the polymer is prone to be damaged by the tip, and the silicon nitride tip can degrade resulting from the contacting with silica[4]. To solve this problem, low stiffness cantilevers must be used to reduce the interaction force and guarantee enough deflection in the meanwhile. Also, the microscope could be operated in the liquid which would reduce the force exerted on the surface by at least a factor of ten[5]. Nonetheless, the liquid may cause the deterioration of polymer (swell or separate from the surface)[4].

2.1.3.2 Non-contact mode

Compared with contact mode, which mainly measures repulsion force due to overlapping of electron clouds, the non-contact mode often detects the signal from Van der Waals interaction (attractive force)[6]. In order to avoid the tip-induced irreversible damage, the tip does not contact the sample surface. Instead, the cantilever will oscillate at its resonant frequency and stay where the amplitude of oscillation is typically a few nanometers (< 10 nm)[7]. In this range (1 nm-10 nm), Van der Waals force is strongest and it tends to decrease the frequency of the cantilever. The signal of the decrease is gathered by a feedback system, which maintains a constant resonant frequency of the cantilever by adjusting the tip-surface distance.

Because of "non-contact", this mode does not suffer from damages both on the surface and tip, that means it will become an ideal method to investigate some soft sample like biological or organic thin film.

2.1.3.3 Tapping mode

Similar to the non-contact mode, the cantilever also oscillates near the resonant frequency in tapping mode. However, it differs principally in that the tip will tap the surface on each oscillation[4]. The oscillation amplitude of tapping mode ranges from 20 to 100 nm, which is much larger than that in non-contact mode. The feedback system detects the signal of oscillation amplitude as well as the changes because of "tapping" and will maintain a constant value of amplitude by adjusting the tip height.

Although the force on the tapping oscillation is higher than that in contact mode, tapping mode still minimizes the damage to the sample surface because of the very short duration of touching. Moreover, lateral dragging force is also dramatically lessened compared with contact mode. As a result, this mode can be widely used in imaging soft and fragile surfaces such as lipid bilayers and single molecule. This method concentrates on the amplitude shift whereas non-contact mode relies on the changes of frequency. Nowadays, tapping mode is the most popular in AFM.

2.1.4 Application of AFM

AFM can be employed in lots of different fields. Obviously, AFM is most commonly used for the imaging process. Besides it, atom manipulation, oxidation, and material transfer can also be achieved by AFM.

2.1.4.1 Imaging

As a general imaging equipment, AFM lets a probe to "touch" and "feel" the sample surface and show the topography. Compared to SEM, another popular imaging technique, AFM has many advantages. Firstly, it has an extremely high accuracy in z dimension (< 1 Å) along with a high simplicity to measure the

sample height. However, one must cut the sample and tilt it to check the profile in z dimension with SEM, which is quite hard to achieve when the pattern is small, and it has a much worse resolution (> 1 nm). Secondly, for the lateral (x-y) dimension, AFM is able to provide an atomic resolution if the sample surface is flat. It is much better than few nm that SEM can reach. Finally, no vacuum environment and conductivity of sample are required for AFM. Air, liquid environment and insulator are both suitable for scanning, thus AFM is cheaper and more available. Nowadays, AFM is widely used in semiconductor and electronics industry. It plays an important role in product inspection to detect the nanometer scale features. Moreover, avoiding a vacuum environment, it is more and more likely to be used for bio-imaging like live cells and tissues.

Unfortunately, it also brings some drawbacks. For the non-flat surface, usually AFM will give a fake sample profile because the probe is hard to reach all the area of the pattern. As a result, vertical structures are shown as slope under AFM. This is called artifacts and is going to be introduced in detail in the following chapter.

2.1.4.2 Particle manipulation

From the invention of AFM, people have shown a great interest in the capability of particle manipulation. However, it took 9 years for AFM to build up an atomic resolution image and another 10 years were spent to develop its capability of particle manipulation. The first report of such manipulation was achieved on Si (111)-(7×7) reconstruction surface. Oyabu and co-workers[8] indicated the possibility to selectively remove adatoms simply by approaching the oscillating AFM tip towards the desired atom. Fig 2.3 shows the results of this nanoindentation experiment. The selected atoms with a circle were removed, leaving a vacancy on the surface. In this process, at least three covalent bonds which fix Si atom to the surface were broken. Furthermore, they showed that one atom attached on AFM tip apex could also be deposited and fill the vacancy.

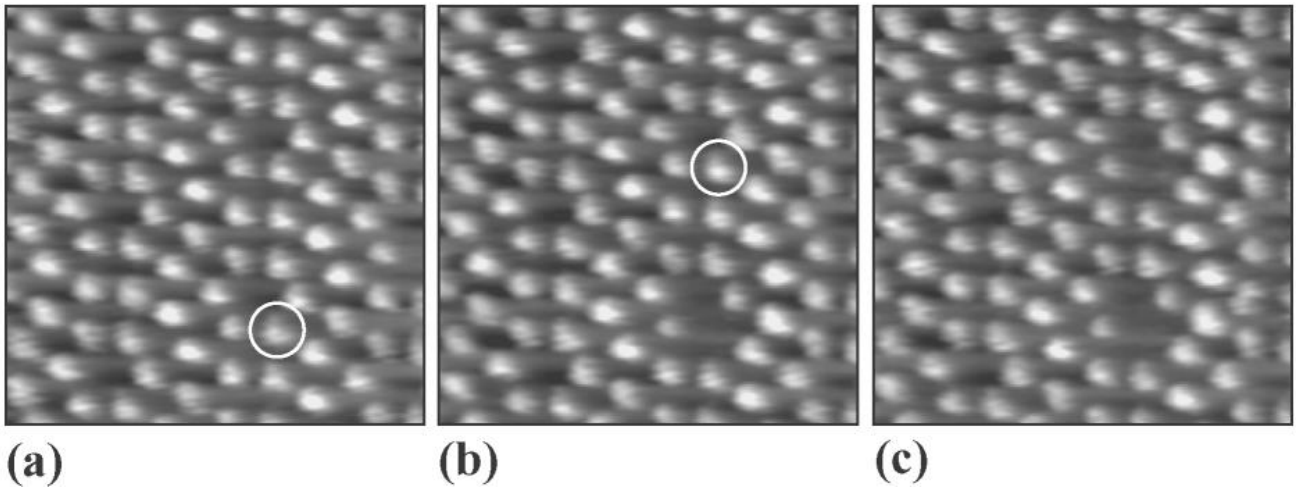

Figure 2.3 Two adatoms on Si (111)-(7×7) surface in (a) and (b) were approached by AFM tip. As a result, two holes were created in (c).[8]

Also, atoms can be moved by the lateral force. When the AFM scan over one atom and the lateral force exceeds the hopping barrier, the atom will jump to another adjacent row, leading to an atom interchange. Fig 2.4 shows some results of such interchange.

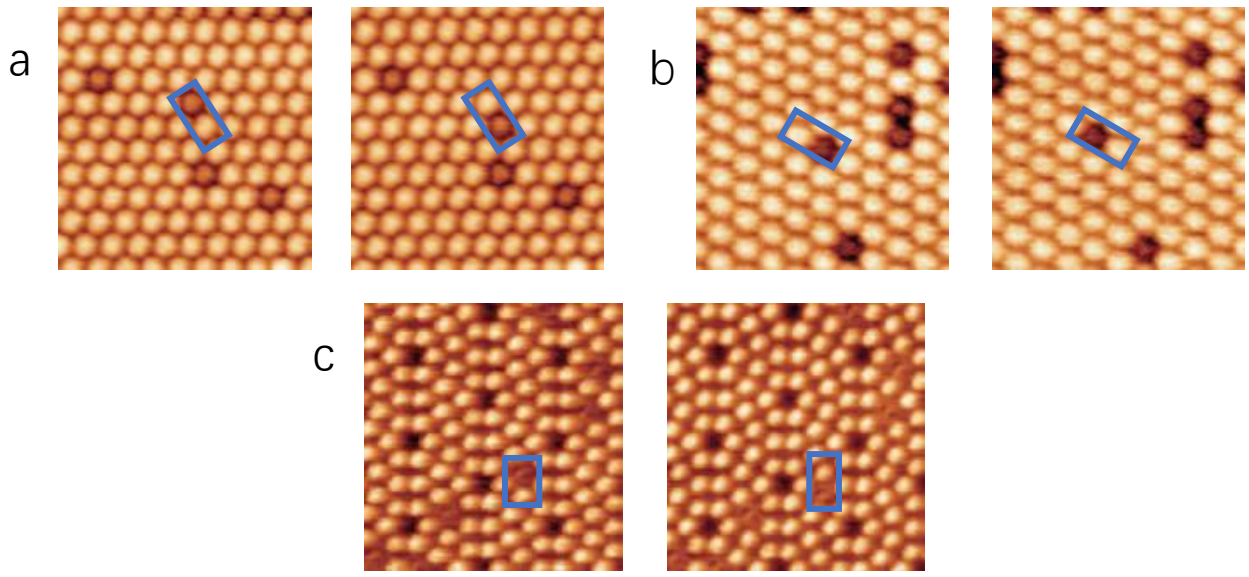

Figure 2.4 Atomic interchange was successfully applied in different surfaces and structures. (a) Sn/Si (111) - (√3×√3) R30°, (b) In/Si (111)-(√3 ×√3)R30°, (c) Sb/Si (111)-(7×7).[9]

2.1.4.3 “Dip-Pen” nanolithography (DPN)

AFM can also be used as a tool to transfer materials and create a pattern on a substrate. The idea is simple: chemical “ink” containing nanoparticles, biomolecules, etc. is attached on an AFM tip and transferred on substrate “paper” by direct “writing”. Although it is not the only direct writing technique, its capability to handle liquids provides a big potential in the field of chemical and bio-application. Fig 2.5 explains the principle of DPN. In a high humidity, a water droplet is formed between tip apex and the substrate surface, which acts as a bridge to connect the material source and desired depositing position.

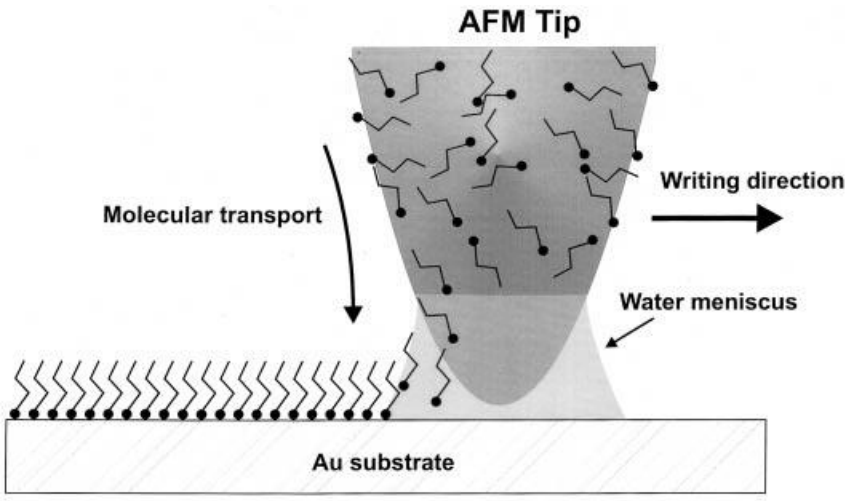

Figure 2.5 Schematic representation of DPN. A water meniscus forms between the AFM tip coated with ODT and the Au substrate. The size of the meniscus, which is controlled by relative humidity, affects the ODT transport rate, the effective tip-substrate contact area, and DPN resolution.[10]

2.1.4.4 AFM Oxidation

This is an electrochemical process. In this technique, the voltage bias is built up between AFM tip and sample, which means that both tip and sample must have some conductivity. When the bias is applied,

hydroxyl is generated from water molecules in the air, becoming the oxidant. As a result, oxides of a few monolayers to a few nanometers will be formed.

The electrochemical oxidation is achieved by non-contact mode AFM.[11] Recently, Davis et al.[12] demonstrated that the AFM oxidation on Al substrate is able to fabricate nano-mechanical CMOS device. In their experiment, a 10 nm oxide line was successfully obtained by AFM oxidation (Fig. 2.6). They also indicated the different results with different parameters (Fig. 2.7).

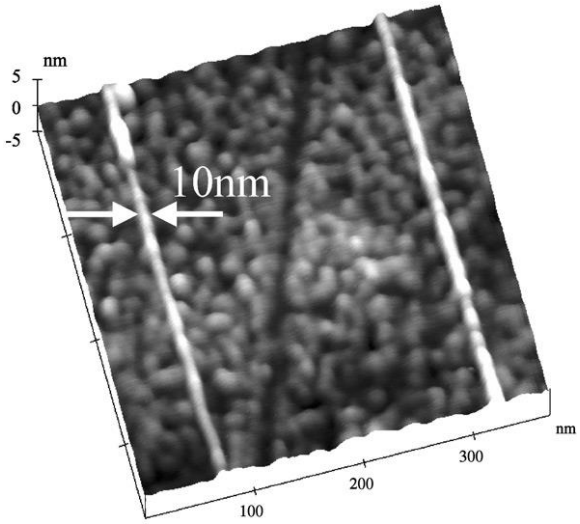

Figure 2.6 Non-contact AFM image of 10 nm wide Al oxide lines on an Al coated SOI substrate.[12]

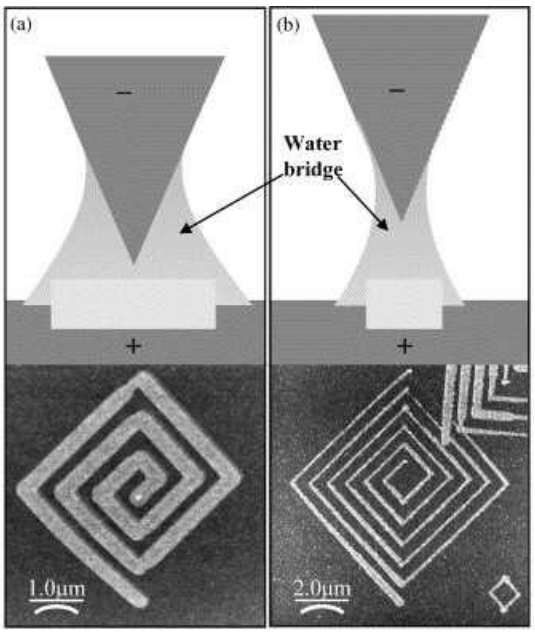

Figure 2.7 Schematic illustration and non-contact AFM image of an oxidized pattern with (a) a small tip/sample distance and high voltage, and (b) large tip/sample distance and low voltage.[12]

2.2 AFM probe

2.2.1 Basic characters

In an AFM, a vital device is the probe, which includes a cantilever with a sharp tip on the end and a holder for easy handling. Also, people usually call it cantilever or AFM tip, using the name of a single part as that of the whole device. Fig.2.8 below illustrates the basic parts and parameters of an AFM probe.

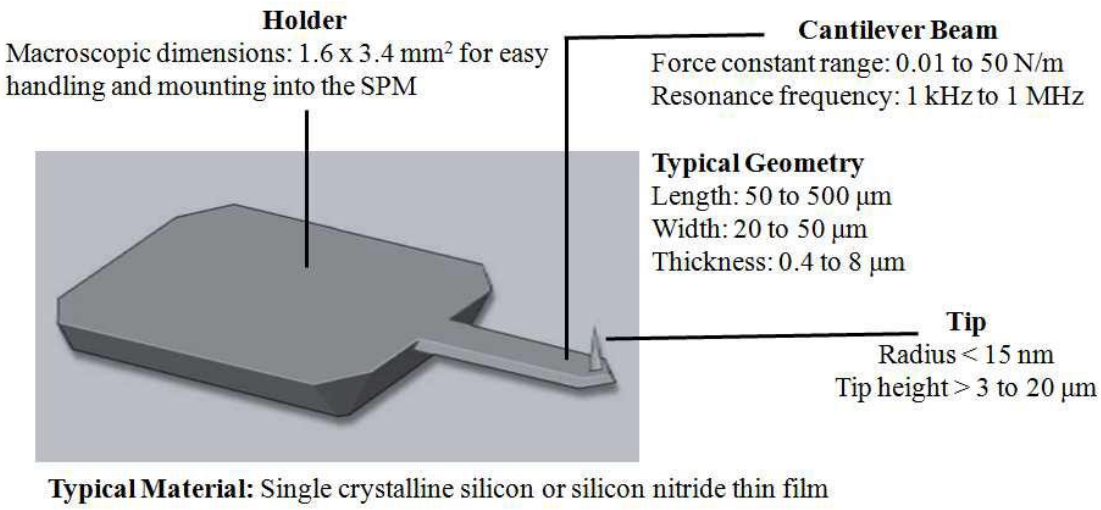

Figure 2.8 Basic characters of AFM probe.[13]

The morphology and material of cantilever contribute to the resonance frequency, which is of great importance in non-contact and tapping mode. The shorter cantilever will have a higher resonance frequency. The tip needs a small radius and large height (high aspect ratio) to minimize the image artifacts and achieve a high resolution.

An AFM probe is produced by MEMS technology. Usually it is made from silicon (Si) or silicon nitride (Si_3N_4). In order to detect various interactions between tip and sample, the probe can be coated by different materials. For instance, the metal film (aluminum or gold) can be coated for increasing the conductivity. Gold could also be used to detect the covalent bond of biological molecules and the interaction with a surface.[14] Also, one may coat some magnetic coatings for investigating the magnetic properties of the sample.

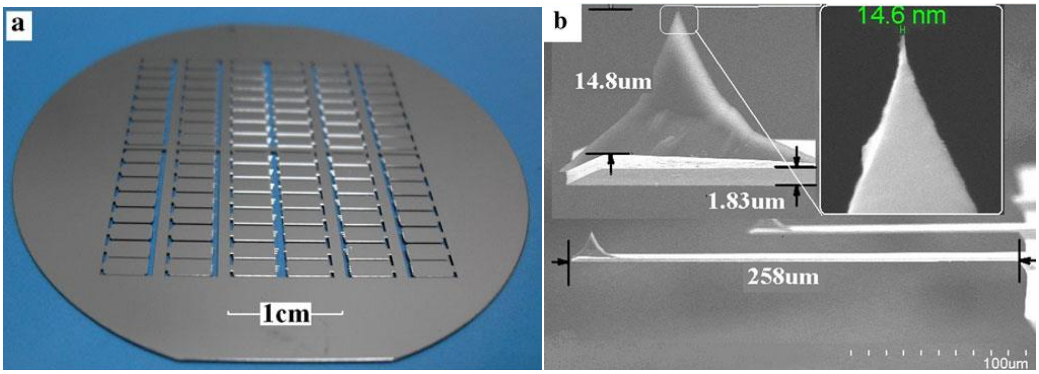

Figure 2.9 AFM probe array (a) and an AFM probe with two cantilevers in (b).[15]

2.2.2 Fabrication of entire AFM probe

AFM probes for imaging are usually made with two materials: silicon or silicon nitride. They are fabricated by two different methods but these methods are both based on KOH wet etching. Also, dry etching can be used for probe fabrication, which provides a better uniformity and reproducibility. After the fabrication of entire probe, people like to do an oxidation sharpening process to effectively decrease the radii of curvature.

2.2.2.1 Fabrication of Si probes

Fig 2.11 illustrates a standard procedure to fabricate a Si probe. The critical advantage that makes it so popular is its simplicity and low cost. KOH wet etch is much cheaper than RIE so that we could avoid using some expensive machines. There are also some restrictions on this method. For instance, the cantilever and tip are both formed by silicon exclusively resulting in the lack of material option. Besides that, the main limit is the tip sharpening. The tip formation will be stopped when the mask falling down. As a result, post-sharpening (oxidation sharpening) must be processed after getting the tip.

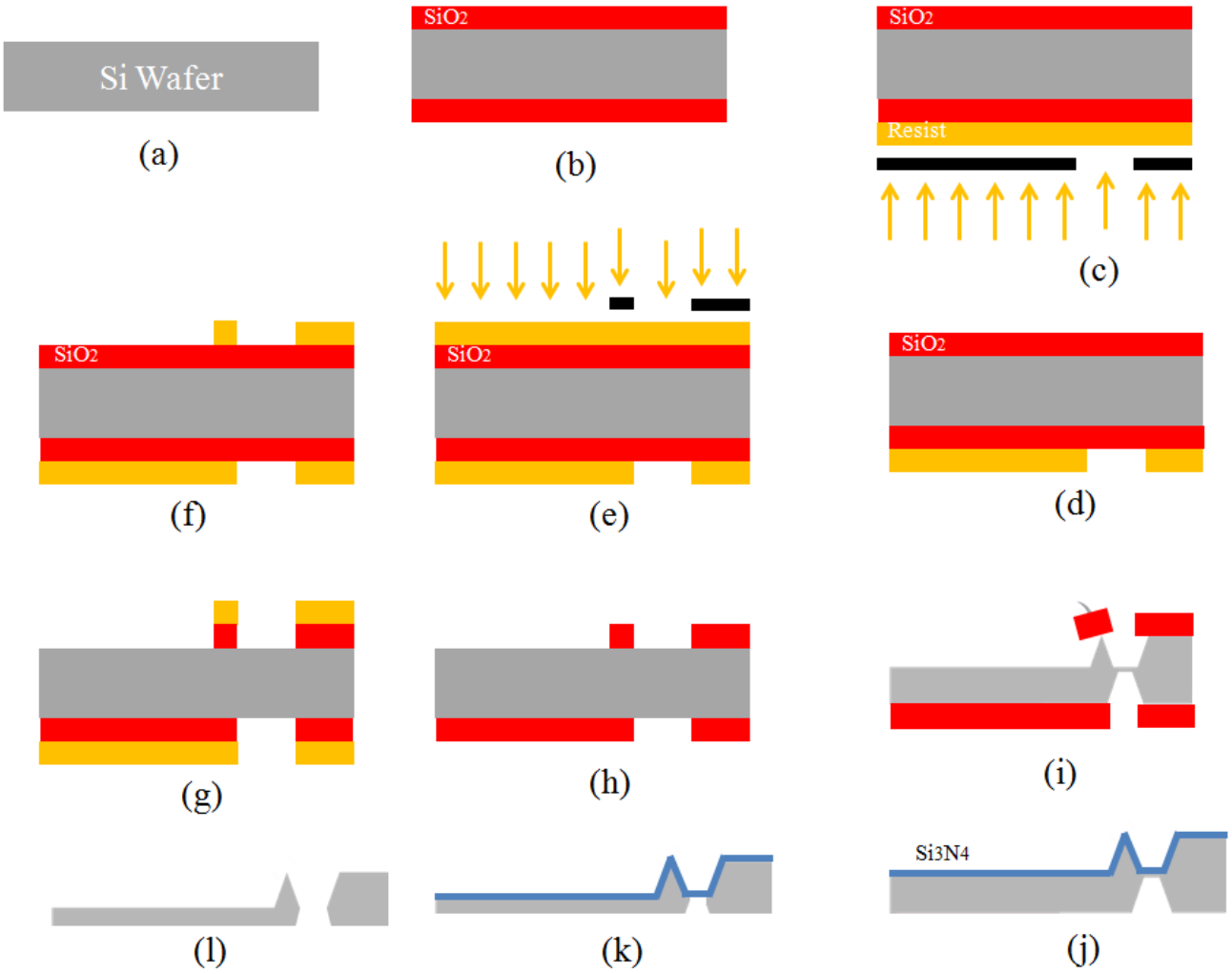

Figure 2.10 Fabrication steps of regular silicon probe. (a) Start with Si wafer (100). (b) Grow SiO_2 on both sides of silicon wafer. (c) Backside photoresist deposition and photolithography (exposure of the photoresist through a chromium/quartz mask) to define the cantilever back shape. (d) Development of the exposed photoresist. (e) Coat photoresist on front side of the sample and photolithography to shape the cantilever top side. (f) Development of the photo resist. (g) Isotropic wet etch to remove the silicon dioxide. (h) Remove the photo resist. (i) Anisotropic wet etch with KOH of silicon. The etching process stops when the etchant reaches <111> plane and the mask (red tilted part) will fall down after the formation of the sharp pyramidal tip. (j) Isotropic wet etch of silicon dioxide and deposition of the silicon nitride layer to protect the tip side of the probe. (k) Anisotropic KOH wet etch of back side. The thickness of the cantilever is determined during this step. (l) Isotropic wet etch of silicon nitride.[16]

2.2.2.2 Fabrication of nitride probes

Fig. 2.11 demonstrates the basic steps to obtain a nitride probe. A critical advantage of this method compared to above one is the wide selection of tip materials. In above method, all parts of the probe are made in the Si substrate; however, in this method, different kinds of materials can be deposited on the Si mold. For instance, robust nitride tips are produced by this technique. Metals, which is conducting can also be deposited to obtain a kind of AFM/STM combination probe. Another significant advantage is that the tip is covered by Si substrate perfectly, avoiding any potential damage until the last step.

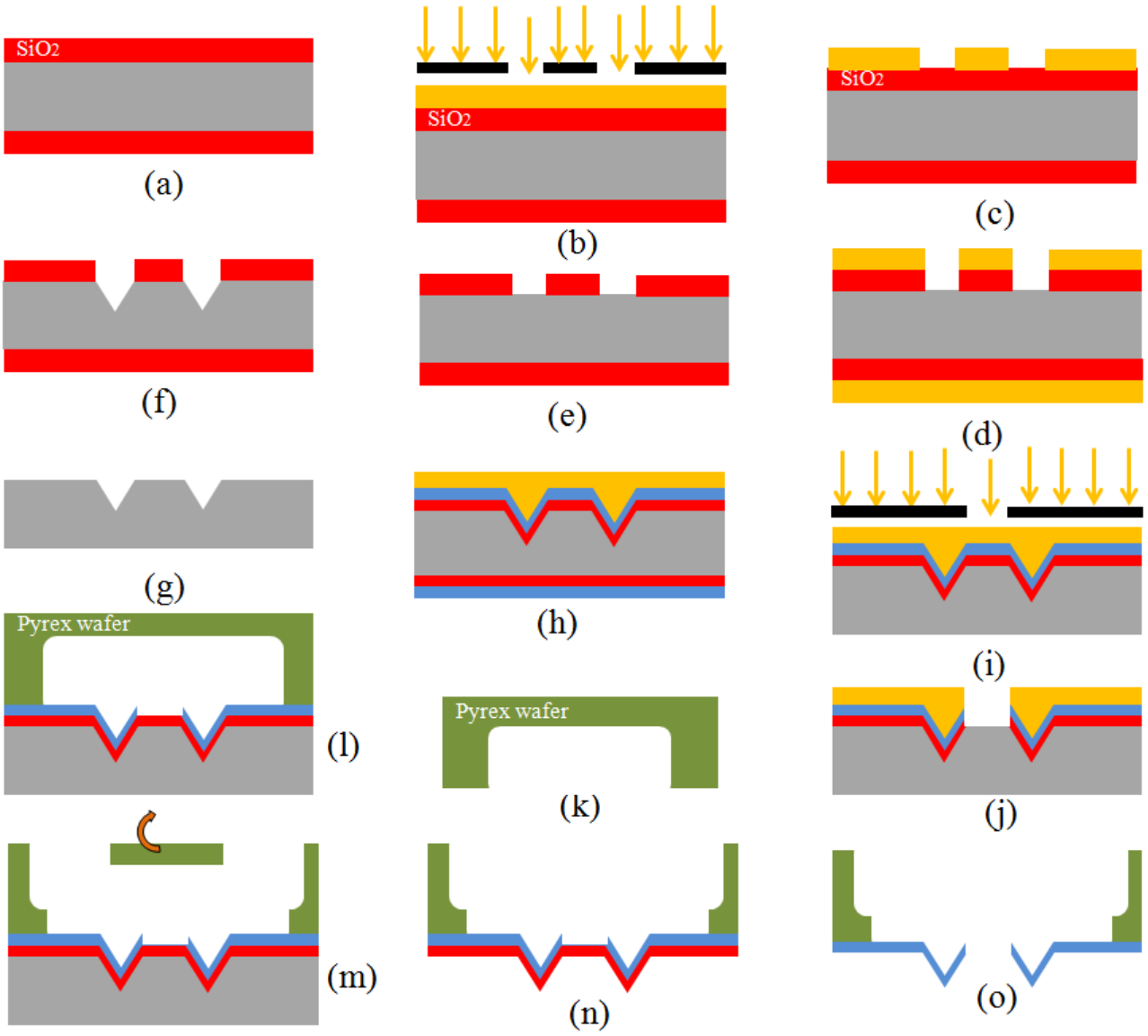

Figure 2.11 Fabrication steps of regular nitride probes. (a) Grow oxide on both sides of silicon wafer (<100> orientation). (b) Coat photoresist and photolithography. (c) Development of photoresist. (d) Coat protection resist layer on back side and etch oxide with buffered hydrofluoric acid (BHF). (e) Remove resist (f) KOH wet etch to of Si. (g) Remove oxide with BHF. (h) Grow oxide, deposit nitride, and coat photoresist on the front side. (i) Remove backside oxide and nitride, photolithography to expose the resist. (j) Development of the resist and etch of the oxide then nitride. (k) Dice Pyrex wafer (to be used as a handle). (l) Anodic bonding the nitride and the Pyrex wafer. (m) Dice and remove unnecessary portion of Pyrex. (n) KOH wet etch of Si. (o) BHF etch of the oxide layer.[16]

2.2.2.3 Fabrication of entire probes based on dry etching

The above two methods are both based on KOH wet etching, which means the tip shape is initially fixed. G. Villanueva and coworkers demonstrated a method to fabricate AFM probe using deep reactive ion etching (DRIE) instead of wet etching. The detailed process is shown in Fig. 2.12. In this method, they fabricated shaft part and apex part respectively by using Bosch process with different gas flow. These two recipes are listed in Table 2.1.

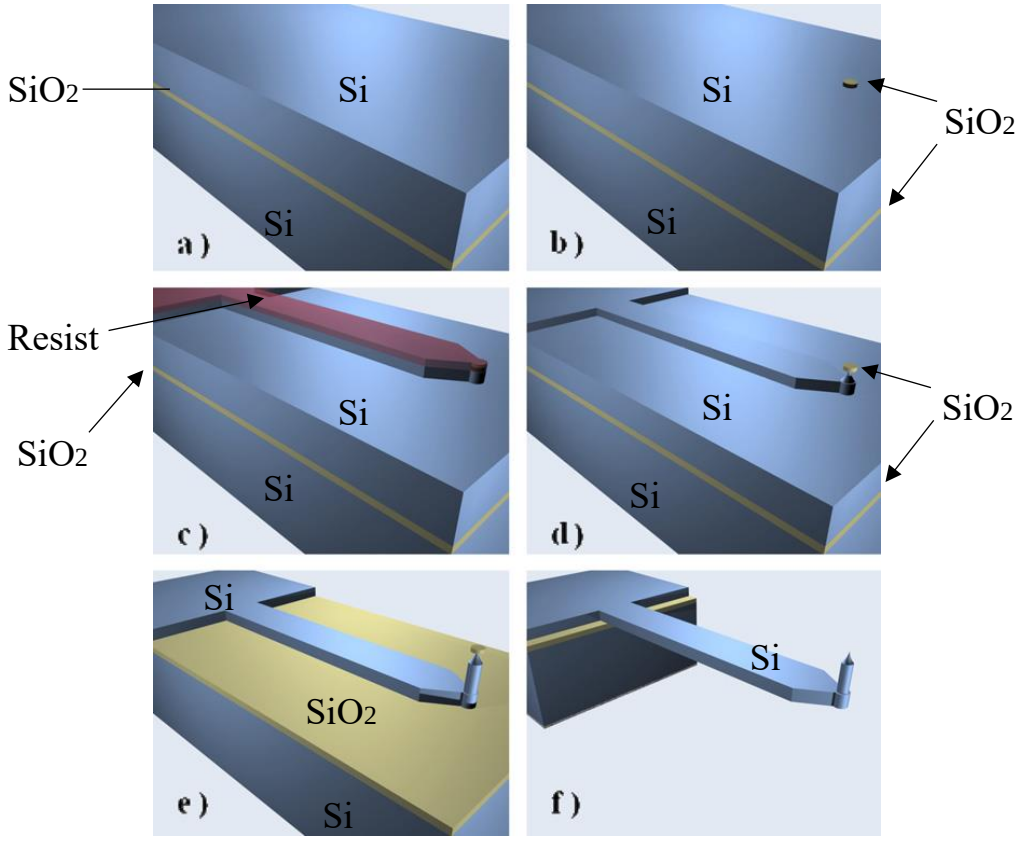

Figure 2.12 The procedure to get AFM probe by deep reactive ion etching (DRIE). (a) Starting from SOI wafer. Top silicon layer is 5 μm or 15 μm. (b) Grow a silica layer and a photolithographic step is used to pattern it, leaving an oxide dot. (c) Deposit a photoresist layer and obtain the cantilever pattern by photolithography. (d) Remove resist, expose the oxide dot and form apex part by DRIE. (e) Fabricate shaft part with a different gas flow in DRIE. (f) Release of the cantilevers by etching the backside silicon layer and buried silicon dioxide.[17]

Table 2.1 Optimized etching parameters. Temperature is fixed at 20 ℃.[17]

Process	SF_6 flux	c-C_4F_8 flux	Pressure (Pa)	Source power (W)	Bias Power (W)	DC Bias (V)
Shaft	150 sccm/2.5 s	100 sccm/1 s	1.4-2.8	1500	15	80-120
Apex	150 sccm/1 s	100sccm/0.33 s	1.6-2.1	1500	15	75-100

2.2.3 Sharpening process

Nowadays, most of the AFM probes are obtained by KOH wet etching, which brings some drawbacks. One is the low aspect ratio. The probe shape is initially fixed and not sharp enough. To increase the sharpness, sharpening process is introduced after the probe fabrication.

2.2.3.1 Oxidation sharpening

One widely used process to sharpen the tip that is produced by KOH wet etching is thermal oxidation. It was first observed by Marcus et al.[18] They found that the oxidation rate of different parts with different curvature of radius is different. The oxidation rate decreases with increasing stress, and the higher curvature, the larger stress. As a result, the oxidation is slower at the apex part of the tip. By repeatedly growing SiO_2 on the Si tips and stripping it with HF, they achieved 1-nm radii of curvature at the tip apex.

Albert Folch et al.[19] used the thermal oxidation to sharpen their silicon tip and compared that with some commercial tips by scanning the KOH-etched 100-nm-deep pyramidal nano pits on Si (100). Fig. 2.13 shows the result. By the oxidation sharpening, the radius of the tip has a dramatic decrease. From Fig. 2.13 (a), all the pyramids appear to have a flat top and end in a ridge rather than a vertex. On the contrary,

the image from Fig. 2.13 (b) shows a totally different result. All the pyramids have a sharp apex because of the sharp tip.

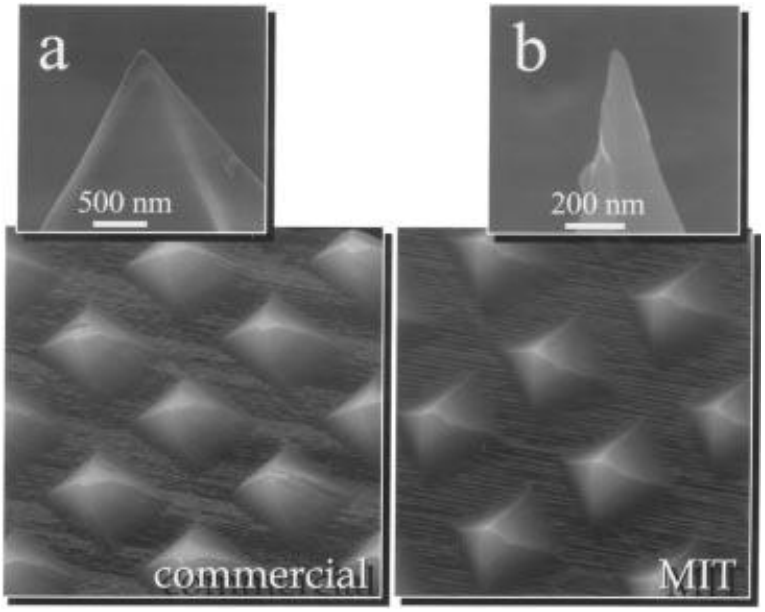

Figure 2.13 SEM images of (top) (a) a commercial tip and (b) a sharpened tip, after acquiring the corresponding (bottom) AFM contact-mode images of 100-nm-deep and 150-nm-side pyramidal pits on Si. The AFM tip irregularities are attributed to wear during scanning.[19]

2.2.3.2 Combination of wet etching and RIE

M.A.R. Alves and coworkers demonstrated a new method employing anisotropic KOH wet etching with isotropic SF_6 dry etching. Fig. 2.14 shows the detailed process and some SEM images are shown in Fig. 2.15. The pyramid shape tip was firstly obtained by KOH wet etching as usual. Then SF_6 plasma was used to decrease the cone angle. Finally, the thermal oxide was grown and removed along with the mask.

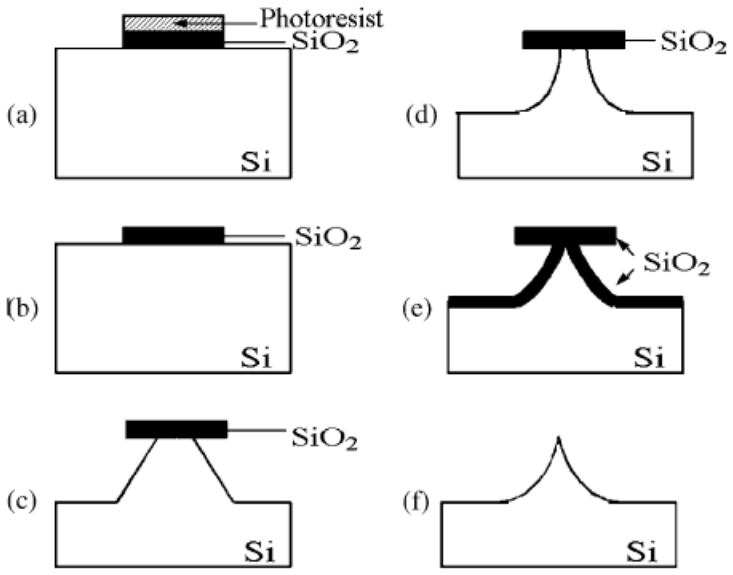

Figure 2.14 Processing steps to form sharpened silicon tips: (a) photoresist pattern is formed on the oxide. (b) Patterned oxide after CH_4 plasma etching. (c) Pyramidal structures formed by wet etching. (d) Silicon tips formed by SF_6 plasma etching. (e) Thermal oxide grown; and (f) sharpened tip.[20]

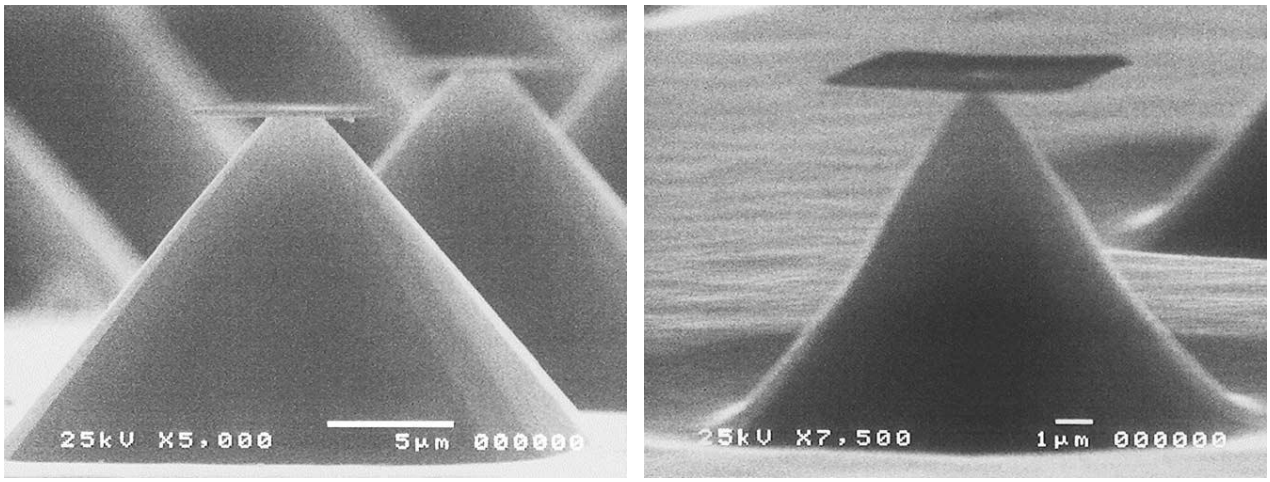

Figure 2.15 SEM image of tip shaped by KOH wet etching (left) and SF_6 plasma etching (right).[20]

2.3 High aspect ratio (HAR) AFM probe

2.3.1 Artifacts when using regular (low aspect ratio) AFM probes

Compared with another popular surface morphology characterization equipment, SEM, AFM has its significant advantages: low cost, easy preparation for the sample, high resolution when the surface is flat. However, when mapping non-flat surface, AFM tip cannot fully follow the complicated structures (steep walls or deep holes), which is called artifacts. Fig. 2.16 simulates the situation when a tip apex scans a rough sample surface. When the dense small columnar structure is sharper than the tip, the surface contour we get from AFM will not reflect the real surface shape, namely, artifacts are resulted by the tip shape.

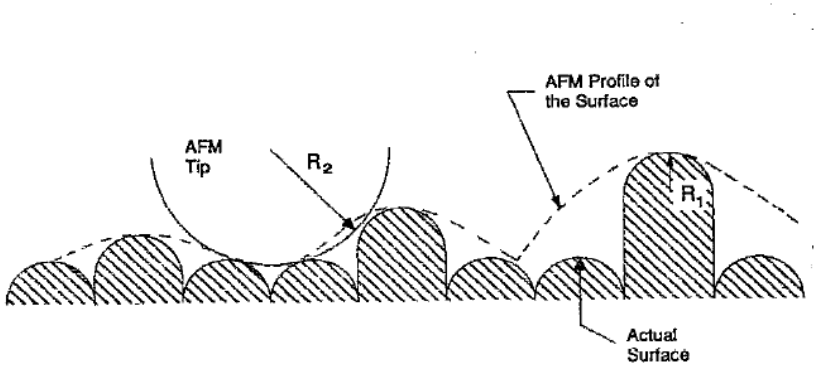

Figure 2.16 A simulation of an AFM tip scanning over a columnar thin film surface. The columnar microstructure is smaller than the AFM tip. The AFM profile is not representative of the real film surface.[21]

It is really hard to scan the sharp structure and steep wall since the tip with a low aspect ratio could not reach the gap bottom. Actually, the image of AFM is a combination of surface structure and the tip shape.

2.3.1 Some methods to obtain high aspect ratio (HAR) tip

Although thermal oxidation is simple to get a sharper tip, which could be used in industry, it does not meet all the requirement. No matter how sharp it is after oxidation, the tip sharp is still the inverse

pyramid which inherits from the initial silicon tip. Thus, lots of researchers are working on methods to achieve a high aspect ratio tip. Fig. 2.17 shows some HAR tips that we can find in the market.

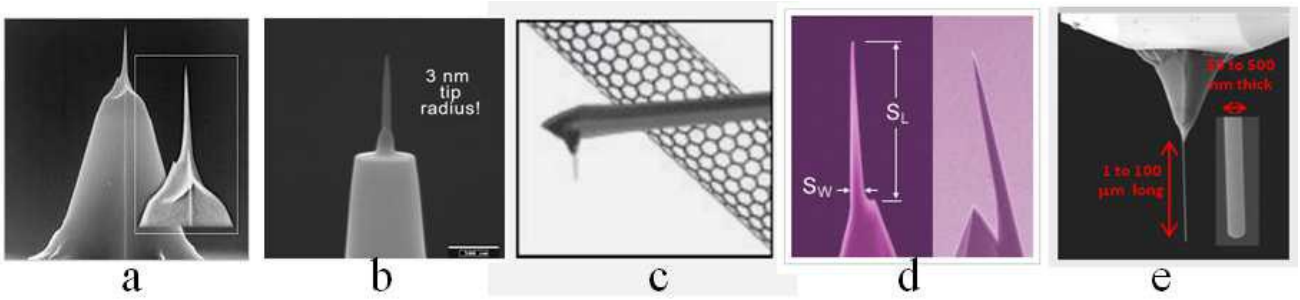

Figure 2.17 shows HAR tips that are currently commercially available. They are made by (a) Focused ion beam milling. (b) Electron/ion beam deposition. (c-d) Carbon nanotube attachment. (e) "Nauga-needle formation" technique. These methods are described in detail in following sections.

2.3.1.1 Focused ion beam (FIB) milling

One method we can easily find is called focused ion beam milling which uses a high energy ion beam to machine the tip directly. This method is simple and straightforward: undesired material near the tip is totally milled and removed by the ion beam, leaving a high sharp pillar in the centre. Fig. 2.18 shows the results. Actually, FIB milling can achieve tips of any shape we want with resolution down to 5 nm and aspect ratio beyond 10:1.

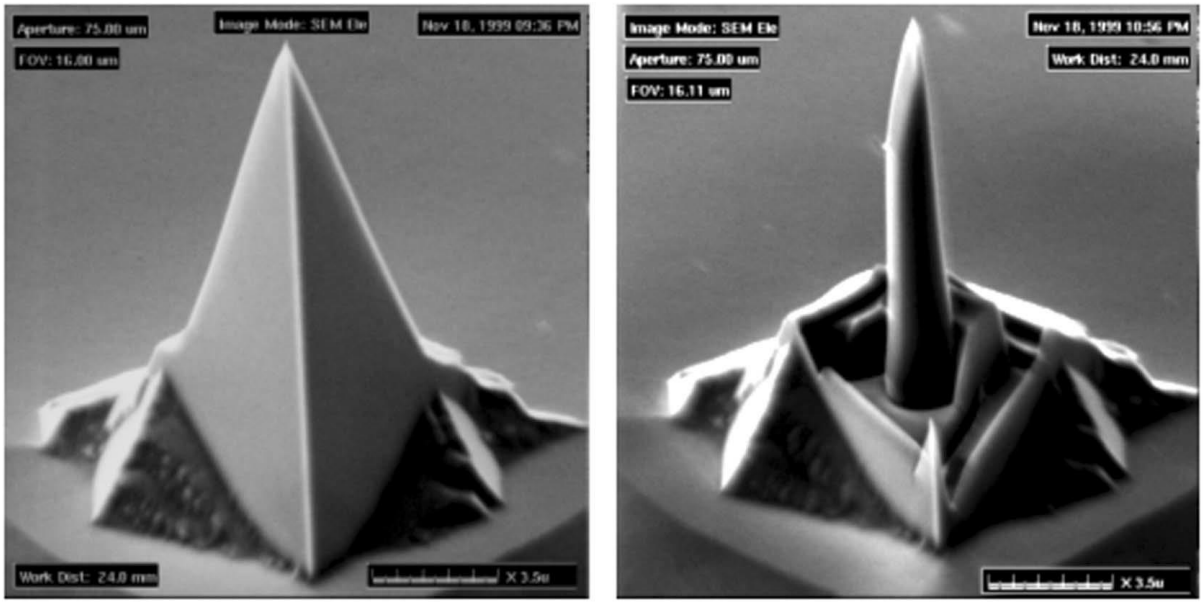

Figure 2.18 AFM probe for tapping mode. (a) The commercial probe with half cone angle of 17º and material of Si_3N_4. (b) The FIB trimmed probe with high aspect ratio.[22]

2.3.1.2 Electron-beam-induced deposition of platinum

Metal-coated tips can enable electrical measurements[23] or they can be functionalized to provide chemical sensitivity[24]. Electron-Beam-Induced Deposition (EBID) is a direct and straightforward way to create an ultra-high aspect ratio tip on the apex of the original pyramid shape (usually the commercial AFM tip).

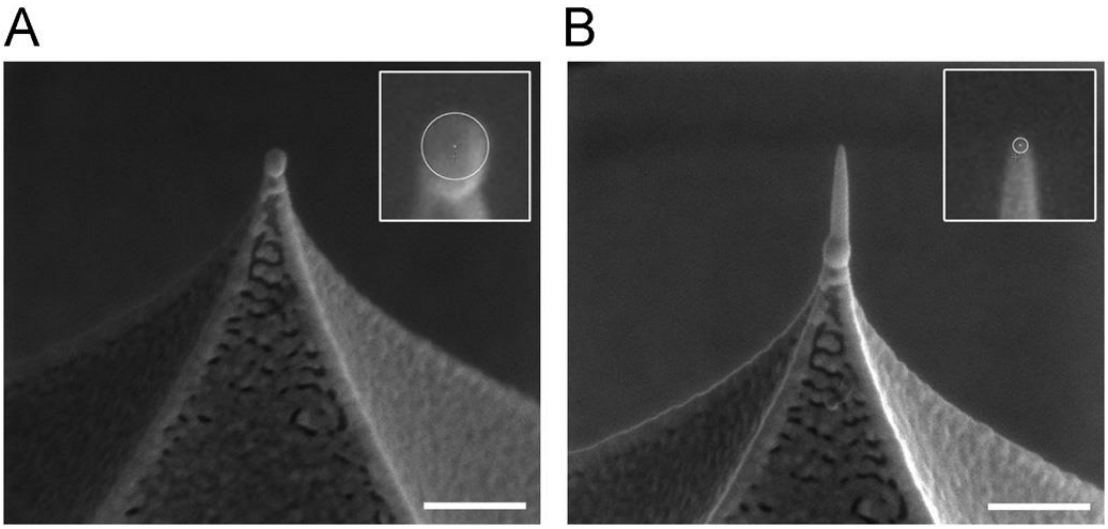

Figure 2.19 SEM images of a commercial OMCL-TR800PB-1 cantilever (A), and the same cantilever following modification by EBID of platinum (B); scale bars: 200 nm.

In the experiment, original AFM tips are aligned and the platinum-containing precursor, methylcyclopentadienyl(trimethyl) platinum IV is introduced through a gas-injection needle. Platinum is inert and has a good biocompatibility. Also, it could be used as electrode material, which makes it a good choice for the deposition. The deposition begins with the reaction between the precursor molecules and the electron beam. By locating the beam at the apex of the original tip and moving the beam gradually upwards, an ultra-sharp, high aspect ratio tip could be formed. The height of tip is controlled by the duration of irradiation. Fig. 2.19 shows SEM images of a commercial cantilever before (A) and after (B) EBID of platinum. The commercial probe dimensions are typical of this model of the cantilever, with ~21 nm, compared with ~4 nm for the EBID-modified probe; in this case, the platinum probe tip has a length of 225 nm and is 30 nm wide at its base (exposure duration of 500 ms).[25]

2.3.1.3 Micro-spot mask and highly selective and anisotropic RIE

Another idea to create high aspect ratio tip is to use the selective and anisotropic dry etching with a mini-mask. Fig. 2.20 (A) shows the process of RIE. Rangelow made the 2 μm-SiO_2 mask layer by RIE in

CHF_3/Ar plasma with vertical sidewalls. $BCl_3/Cl_2/Br_2$ plasma has been used to etch the silicon.[26] Optimizing all the conditions (such as RF-power and pressure) to present a high selectivity (Si: SiO_2 = 60:1), finally, high aspect ratio tips shown in Fig. 2.20 (B) were be obtained.

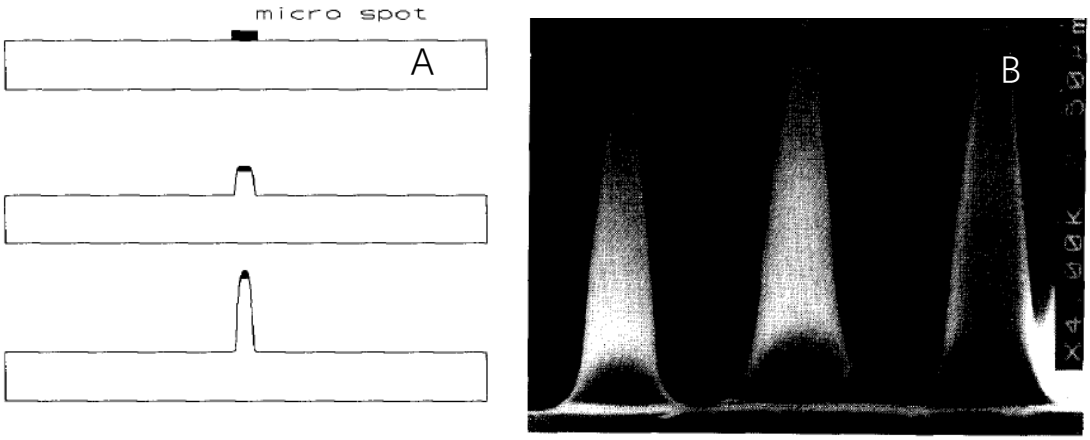

Figure 2.20 Tip fabrication sequence by micro- spot mask and highly selective anisotropic etching.[26]

2.3.1.4 Carbon nanotube (CNT)

Carbon nanotube (CNT) is an excellent material for AFM tip because of its unique structure and properties. Carbon nanotubes consist of a honeycomb sp^2 hybridized carbon network that is rolled up into a seamless cylinder, which could have a micrometer length with a nanometer diameter. Such ultra-high aspect ratio ($10–10^3$) provides the ability to reach the bottom of some steep structures. Also, the small radius of curvature (less than 10 nm) significantly increase the lateral resolution of the tip.[27]

Carbon nanotube tips were first produced in 1996.[28] Two kinds of CNT can be used in AFM tip: single-walled nanotubes (SWNT), which have only one shell and typical diameters of 1–3 nm; and multiwalled nanotubes (MWNT), which have multiple concentric cylinders with typical diameters of 5–100 nm.[29] Usually, the CNT is attached on the surface of a silicon probe (shown in Fig. 2.21). Thus, characters to describe a CNT tip are its length, radius, and orientation (angle with respect to the surface, θ).

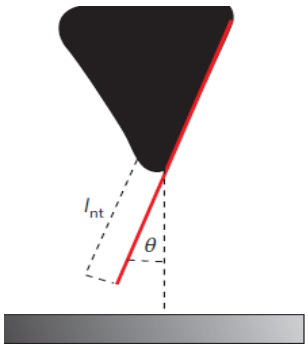

Figure 2.21 Nanotube tips are characterized by their length and angle relative to the surface. There are several methods to grow a CNT on the AFM probe.[29]

The first CNT tip was made by direct manipulation. The original silicon tip coated with the adhesive touch a small bundle of MWNTs, and one CNT was picked from the bundle to attach on the silicon probe. It is the simplest method to form a tip, however, it is hard to be scaled up to meet the requirements of industry.[29]

After 1998, a breakthrough was made that the chemical vapour deposition (CVD) can be used for the growth of MWNT tips and then SWNT tips [30]. The schematic shown in Fig. 2.22 illustrates the principle. The CNT attached will follow the edge of the original tip and finally grow on the apex.

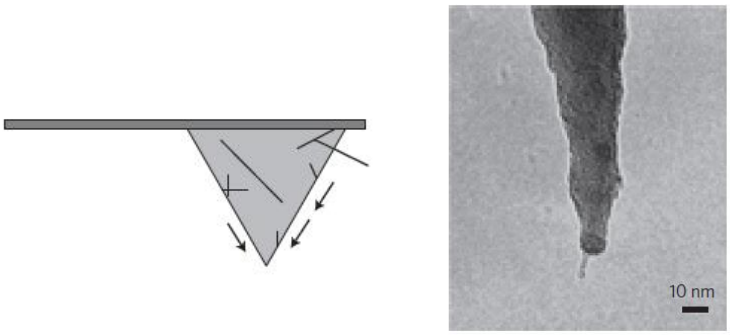

Figure 2.22 Surface growth CVD nanotube tip preparation. Left: Schematic of the growth process. Right: TEM image of an individual SWNT tip produced using this technique.

A critical advantage of this process is easy to batch fabrication. All the characters (length, diameter, and orientation) are possible to be controlled well. However, it still has a severe drawback. The fragile CNT

tip is much easier to be broken after scanning compared with the silicon tip. As a result, CNT tips are still not popular nowadays. We will focus on silicon tips in the following chapters.

2.3.2 Our method

We can find the truth easily that above methods like FIB milling or electron beam deposition can only machine HAR tip one by one, leading to a low throughput and high cost. Obviously, to increase the throughput and reduce the cost, batch production process is the most effective and efficient way. Here we report a new process to form a mask dot on the apex of the tip. This is a lithography-free process. This dot is then used as the hard mask in Inductively Coupled Plasma – Reactive Ion Etching (ICP-RIE). The whole process is based on thin film deposition and etching and can be achieved in batches. This will be introduced in detail in Chapter 3.

2.4 Conclusion

In this chapter, we reviewed the history, principle, and application of AFM. Since the invention of AFM, it has provided a low-cost method with high resolution to characterize sample surface. The essential part AFM is the probe. Nowadays, AFM probe is made with silicon or silicon nitride. Both are based on KOH wet etching. Some probes can also be fabricated by plasma dry etching. Right after fabrication all these probes are not as sharp as we want, so sharpening process, especially thermal oxidation sharpening is widely used. However, the aspect ratio of the tip is still not high enough even after sharpening, leading to a severe problem called artifacts. To solve this, high aspect ratio tips were developed. HAR tips can be obtained by several ways such as FIB, EBID, and CNT, but none of them can achieve batch process and strong tips in the same time, which leads to a high cost. We introduce our new method to batch fabricate silicon HAR tips in order to obtain a high throughput and low cost.

Chapter 3. Batch fabrication of high aspect ratio silicon tips

This chapter describes in detail our method to develop the high aspect ratio silicon tips by nanofabrication process in batch. The main advantage of our method compared to other commercial HAR silicon tips is batch fabrication process, whereas other methods all fabricate the tips one by one.

3.1 Background

One of the most important parts of Atomic Force Microscope (AFM) is the AFM probe. When the AFM tip feels the sample surface, blunt and low aspect ratio tip cannot reach to the deep trench of the HAR pattern in the samples (such as steep sidewall and deep hole), which leads to unfaithful information about the sample. In addition, a high aspect ratio (HAR) tip is required to get the high vertical resolution of the nanostructure. Notably, most commercially available HAR tips are produced one by one using focused ion beam milling (FIB) or electron beam induced deposition (EIBD) and a few other methods, leading to low throughput and high cost ($100- $500 per tip, 20 times that of regular tips). To reduce the cost, the best way is to go with the batch fabrication process.

Our method starts with regular pyramid (thus, low aspect ratio) tips called “All in One tip”, which are commercially available in the market, and then those were employed, in batch, to produce high aspect ratio pillars on the tip apex. A very high and dense pillar array sample was used to test our tips since this pillar array sample is really hard to characterize by using regular low aspect ratio tips.

3.2 Fabrication process to make the HAR tips

The basic logic of our process is simple and straightforward: create a small mask dot on the tip apex and do Si etch to form a high aspect ratio pillar on the tip apex. Thus, the whole method is divided into

the three steps: evaporation of masks, etching to form small dot-like etching mask and then Si dry etching to create the long pillar.

3.2.1 Shape of original tips

We started from commercial tips called “All in One” tips purchased from BudgetSensors®, which have a typical pyramid shape.

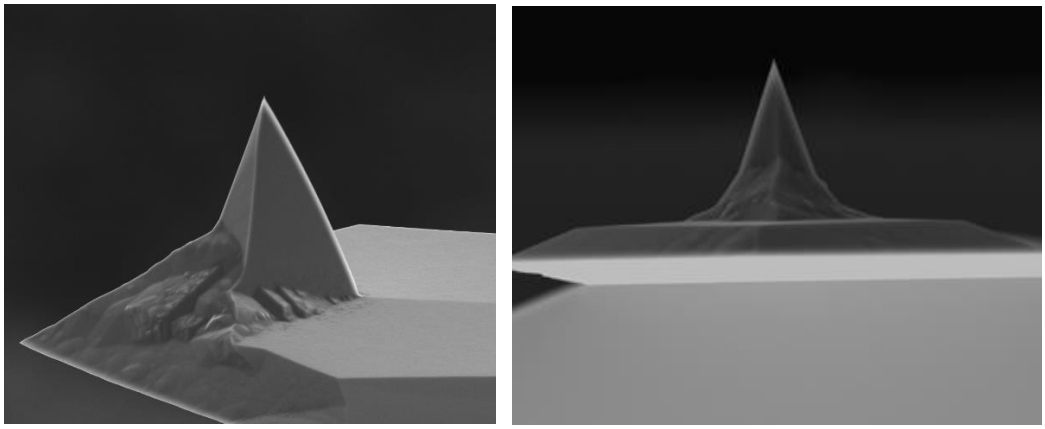

Figure 3.1 SEM images of original tips. (Left): side view, along the cantilever. (Right): back view.

3.2.2 E-beam evaporation of masking materials

Regular evaporation is not capable of depositing small dot directly on the tip apex because the materials would cover the whole area of tip unless there is shadow effect. Here, we implement angled evaporation technique to deposit double mask layers. Firstly, we coat 30 nm chromium oxide (Cr_2O_3) film on one side of the pyramid. Then, a second layer, 70 nm Aluminum (Al), is coated from another side. As a result, these two materials cover two different sides of the pyramid but have overlap only on the apex. This means only a small amount of Cr_2O_3 is covered and protected by Al layer and this will form the small dot in the next step. In this evaporation process, 20-50 probes can be mounted on a carrier wafer, thus a batch process is implemented.

There are several parameters that should be considered in this process. Firstly, the materials used as masks must meet the following three requirements. One is the cost. The materials should be cheap and commonly used. Another requirement is they can be evaporated by e-beam evaporation technique and coated on probes. Last but not the least, they should have a low residual stress in order to cover and protect the probes without peeling off. In theory, thin film deposition usually has three kinds of residual stresses: intrinsic, thermal and external. Intrinsic stress is due to the properties of the material itself like atom spacing and grain orientation, and is usually generated during the growth of the thin film. Thermal stress is created because of different thermal expansion coefficients between the substrate and thin film. External stress is considered as a sum of outside stress applied to the system.[1, 2] These stresses have a large impact on our process. In the beginning, we chose Chromium (Cr) and Aluminum as masking materials, which are both cheap and readily found. However, Cr was not a suitable mask due to its having a large stress. Zheng[2] from our group deposited these two materials on an AFM probe and tested them by Si plasma dry etching. Results are illustrated in Fig. 3.2. We can easily find that Cr tends to have a large stress that distorts the mask layer. As a result, AFM probe was not covered perfectly by the mask and exposed to the etchant. In the meantime, Al showed a good performance to protect the sample underneath. Abandoning Cr, we found another material, chromium oxide (Cr_2O_3), which is widely used in green coating and is very cheap. Cr_2O_3 performance is pretty similar to Cr during ICP plasma etching and wet etching processes, so as to we didn't need to change any parameter of the etch recipes. More importantly, Cr_2O_3 has a low stress like Al and would not distort the mask layer. At last, we chose Cr_2O_3 and Al as masking materials.

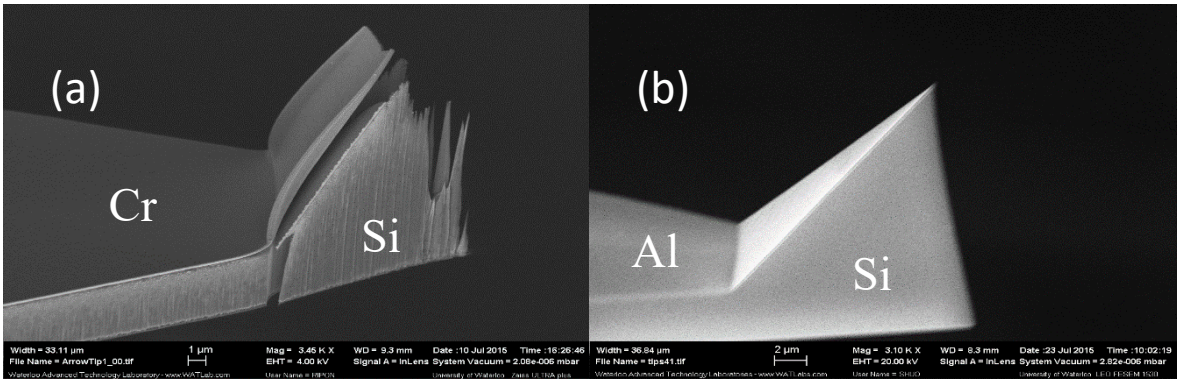

Figure 3.2 The SEM images comparing the results of protective layer consisting of (a) Cr, (b) Al. It is clearly seen that large stress distorts the Cr layer and the unprotected regions of silicon are damaged during plasma dry etching in the next step. On the contrary, Aluminum is competent to keep the tip well-protected.[2]

Then, we consider the film thickness of both mask layers: Cr_2O_3 and Al. For Cr_2O_3, it will be the etch mask in the Si dry etching, thus the selectivity between Si and Cr_2O_3 should be very high. By measurement, the selectivity for the dry etching recipe we used is more than 100:1, which means only 1 nm Cr_2O_3 would be consumed while 100 nm Si is etched away. Since we hoped to have a 1.5 μm pillar on the top, 15 nm Cr_2O_3 on apex is needed at least. On the other hand, Al thickness can vary in a range instead of an exact set value. Al is used as a sacrificing layer to protect Cr_2O_3 on the apex, therefore the only requirement of Al is that it is thick enough to protect Cr_2O_3 (but too thick Al will more likely cause overlap with Cr_2O_3 on the two side-ridges). In practice, our deposition thickness of Al is roughly 70 nm.

3.2.3 ICP plasma etch of chromium oxide

Because we only require a small dot-like etch mask on the tip apex, Cr_2O_3 coated in other areas should be removed. There are two common ways to remove materials. One is called wet etching, which uses chemical solutions to etch materials desired. The counterpart is dry etching, which generates plasma in the etch chamber. We firstly abandoned wet etching technique because it is the isotropic etching. Fig. 3.3 shows the lateral etch (isotropic) of wet etch and reactive ion etching (RIE). In wet etching, liquid solutions are used so the etchant arrives and attacks sample isotopically. As a result, a severe

undercut may be created. For our process, Al layer cannot protect Cr_2O_3 from the liquid etchant and no Cr_2O_3 will remain on the tip apex. On the contrary, dry etch has the capability to achieve anisotropic etching. Reactive Ion Etching (RIE) is the most popular dry etching method in the semiconductor industry. It generates plasma including ions and radicals. For some cases, the whole etching process is controlled by radicals (chemical etching), resulting in the isotropic etching profile. There are two mechanics to achieve anisotropic etching. First, ions are driven by built-in bias to cause ion bombardment (physical etching). Ion bombardment disrupts un-reactive sample surface and creates a damage layer on the unprotected horizontal area (much less damage to the sidewall), helping and enhancing reactions between sample and radicals. Second, in plasma, some monomers such as CF and CF_2 will be generated. When they are absorbed by silicon surface, polymerization happens and the sample surface is covered by a protective polymer layer. Ions coming in vertically removes polymer layer on the horizontal surface whereas the sidewall is still covered. Because of these two mechanics, vertical profiles can be obtained.

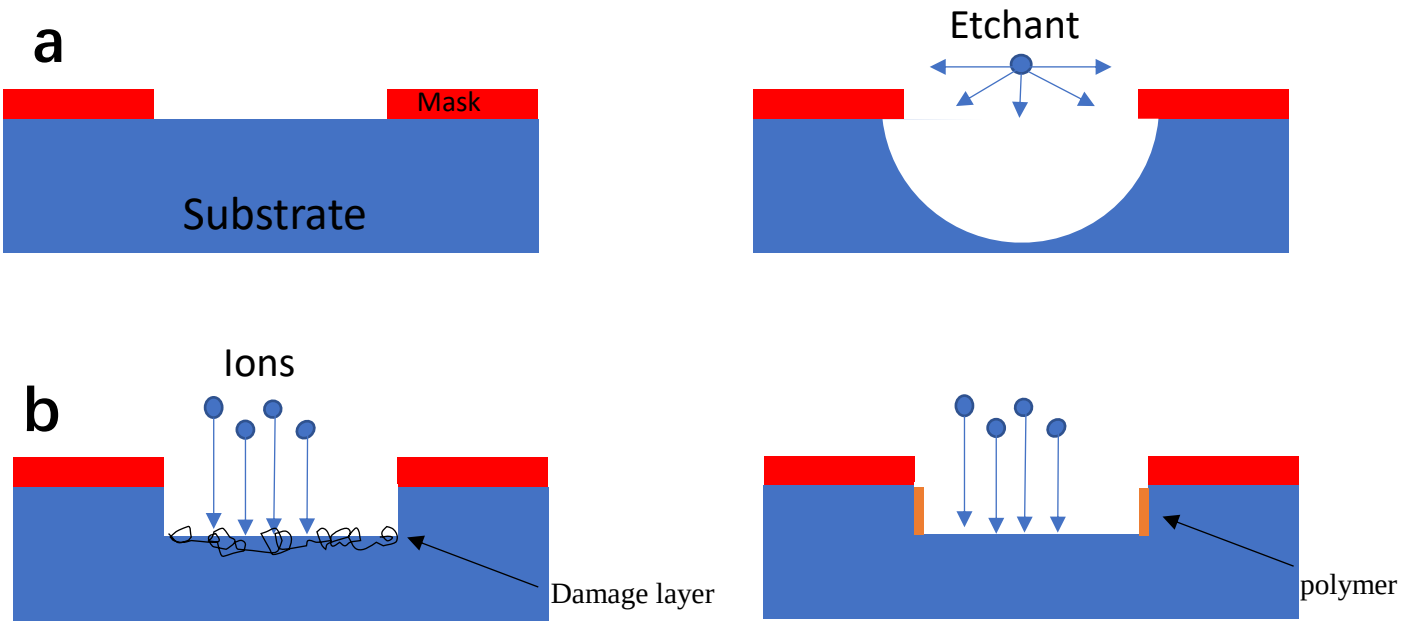

Figure 3.3 Etching profile for (a) wet etching, and (b) ICP-RIE (Reactive Ion Etching). Wet etching makes the isotropic profile and materials under masks will also be attacked. On the contrary, RIE can obtain a vertical etching profile because it is assisted with ion bombardment which occurs in one direction.

Once we determined the etching method, we need to select the etching recipe. One popular recipe to etch Cr is chlorine (Cl_2) gas mixed with oxygen (O_2) gas. The recipe we chose was created by Ripon from our group, University of Waterloo. The gas ratio is Cl_2:O_2= 50sccm:5sccm. Plasma will react with Cr to form volatile CrO_2Cl_2 which can be removed easily. As we said before, the etch performance of Cr_2O_3 is very similar to Cr in RIE so we didn't change any parameters for Cr_2O_3. However, Al will also be etched in this recipe because Cl_2 attacks Al to form volatile $AlCl_3$. Therefore, selectivity must be studied in this case. We firstly coated 100 nm Cr_2O_3 and 100 nm Al on two small Si wafer pieces respectively, then mounted them on a carrier wafer and did the RIE. After one-minute etching, we covered a small area of them with a drop of photoresist and etched uncovered areas by wet etching. Stripping the photoresist by acetone, we got a small area of Cr_2O_3 or Al on Si substrate. After measuring the height of Cr_2O_3 and Al layers, we got the etching rate as 75 nm/min for Cr_2O_3 and 35 nm/min for Al. These rates are only for a horizontal surface, not a tilted plane. The selectivity was around 2. Because we have 70 nm Al compared to 30 nm for Cr_2O_3, Al was thick enough to protect the Cr_2O_3 in the whole etching process.

3.2.4 Wet etch of Aluminum

As said before, wet etch is isotropic but has a very high selectivity. For our case, Al works only as a protection layer and no pattern transfer is needed using Al as a mask, so the only thing we need to care about is removing the Al layer eventually. Comparing wet etch with dry etch, we found that dry etch is not suitable since it will damage Cr_2O_3 as well. On the contrary, wet etch would only etch Al benefiting from the high selectivity, thus wet etch is an ideal choice in this step.

To etch Al, there are two classical etchants: PAN and hydrofluoric acid (HF). In the beginning, we chose HF because HF has a high etch rate at room temperature. PAN etchant, a mixture of phosphoric acid, acetic acid and nitric acid, doesn't work so well at room temperature and usually people like to heat it up to 40°-50° to have a suitable higher etching rate. However, HF has a drawback: it is extremely dangerous and may cause death when using mistakenly. We tend to avoid HF when substitute exists.

In our case, Al is a very thin layer (70 nm) and will be thinner after RIE. Although the etching rate of PAN is lower than that of HF, the total etching time will not be too long. As a result, we finally chose PAN as the etchant to etch Al.

After selection of the Al etchant, a visual test was taken to measure the etching rate approximately. We deposited a thin film of Al on a small piece of Si and immersed it in PAN solution. Because Al has the shiny silver color which looks so different from that of Si, we can see Al disappearing gradually in the solution. We counted the total duration of etching and obtained the etching rate of 70 nm/min at 40 ℃. This method is very rough and the etching rate is not accurate, but PAN will not attack Cr_2O_3 or Si, and thus the etching time can be doubled to ensure all the Al is etched away. Finally, we set the etching duration to be 2 minutes.

3.2.5 ICP plasma etch of Silicon

After etching of Cr_2O_3 and Al, a small Cr_2O_3 dot is formed on the tip apex, and the last step is etching Si to create a high aspect ratio pillar on apex. Pillar means we only want etching to happen in vertical direction with Cr_2O_3 as a mask. In other words, selective anisotropic etching (RIE here) is required. Nowadays, the most popular recipe to etch Si is Bosch process, which switches C_4F_8 and SF_6 to run polymerization and etching process in a cycle. Because Bosch is a kind of non-continuous process, the sidewall always has a wave-like profile (shown in Fig.3.4) In order to obtain a smooth sidewall, we employed a series of non-switch recipes, which continuously inject C_4F_8 and SF_6 with a constant gas flow ratio.

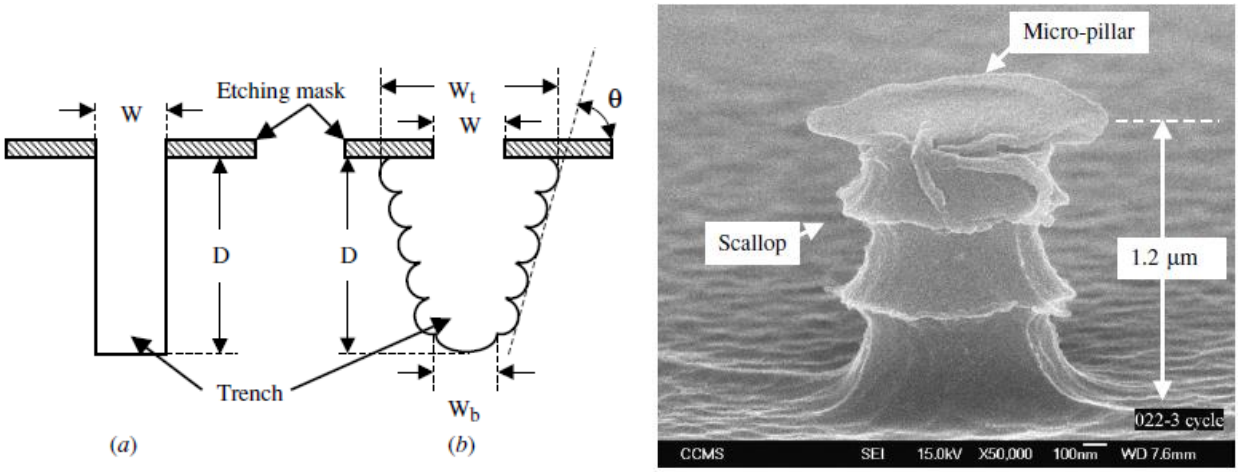

Figure 3.4 Left: Ideal profile (a) and real profile employing Bosch process. Right: SEM image of a pillar etched by Bosch process.[3]

3.3 Results and discussion

3.3.1 Etched tips profile

Our method provides a simpler way to achieve batch fabrication of HAR probes. Here we present the results followed by all steps of the fabrication. Fig. 3.5 shows some SEM images of our tip. A high aspect ratio pillar is successfully created on the apex of the tip. This pillar is more than1.3 µm long, has an 80-100 nm diameter for the body part and less than 10 nm radius of curvature. To make sure it is a real pillar, we have taken some images from the back side (Fig. 3.10c) as well, because some tips seem to have a pillar apparently but actually it is not when viewed from the other side (Fig. 3.11). Only when we see the pillar-like structure from both viewing directions, we can say it is a high aspect ratio tip with no doubt.

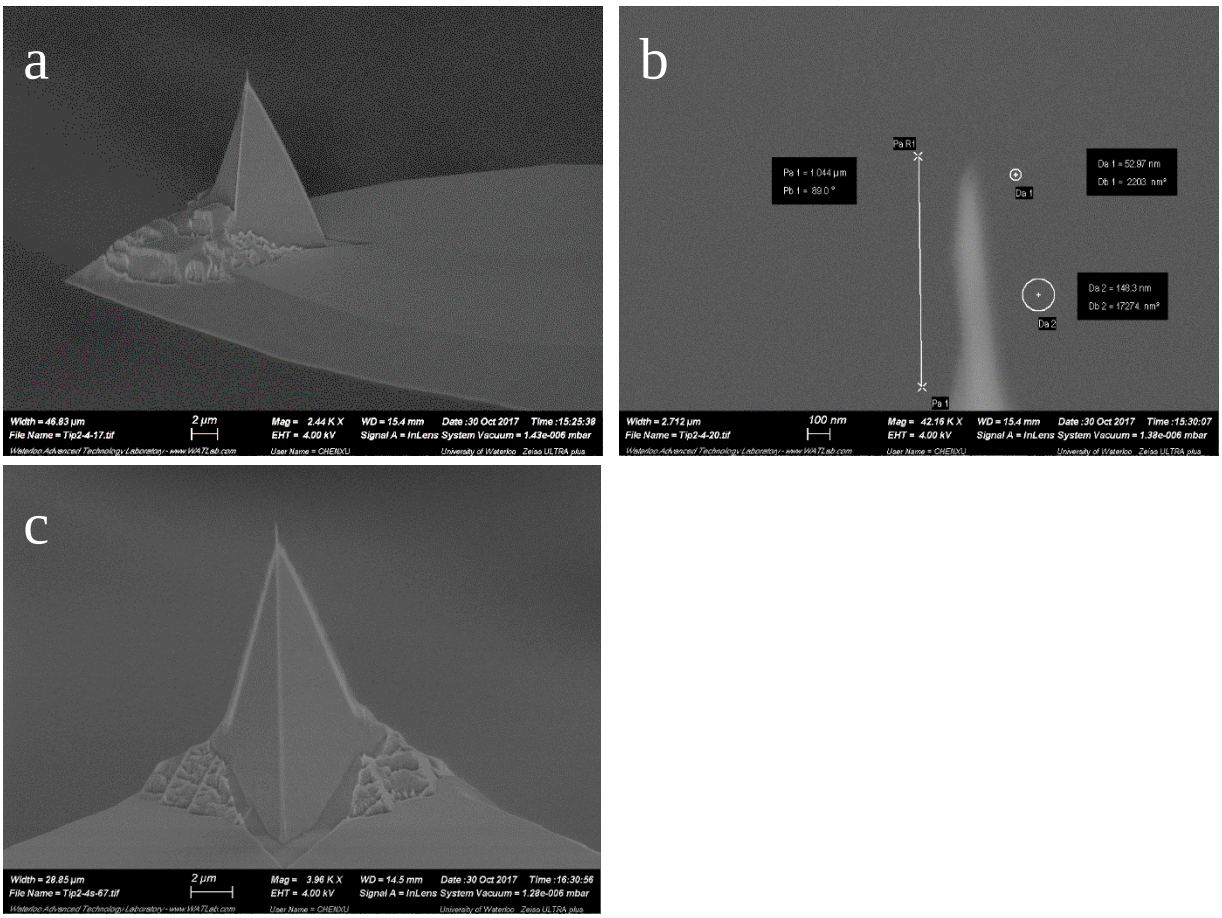

Figure 3.5 SEM images of side view of HAR probe (a), zoom-in image of apex part (b), and backside view of the same probe (c).

Since our method is a batch process, here we mounted 28 tips in one batch and fabricated them in the same time. In SEM characterization, most of them (21/28 tips) had good profiles, which are shown in Fig. 3.6. The pillar diameter was 80-100 nm and radius of curvature of the tip apex was less than 10nm.

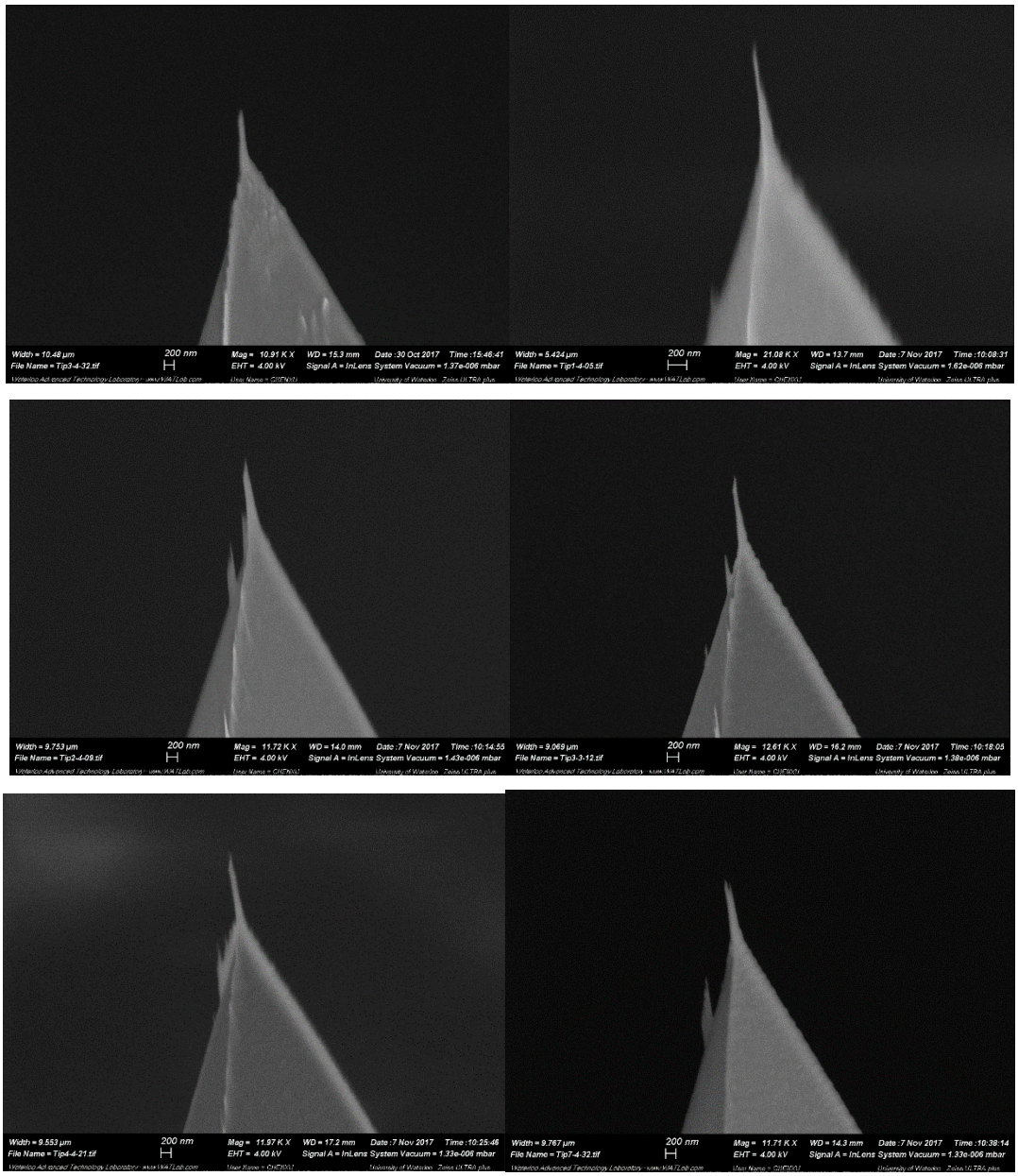

Figure 3.6 SEM images of some fabricated HAR tips.

3.3.2 Imaging using our HAR tips

To test the performance of our HAR tips, we have prepared a pillar array sample. (Fig. 3.7) All pillars have 400 nm height and 200 nm diameter. The period of the array (center to center distance of the closest circles) is 400 nm. AFM tips have to scan 200 nm wide and 400 nm deep gaps of this sample, which is challenging for regular commercial tips. We scanned the same area of our sample by a regular tip and one of our fabricated HAR tips.

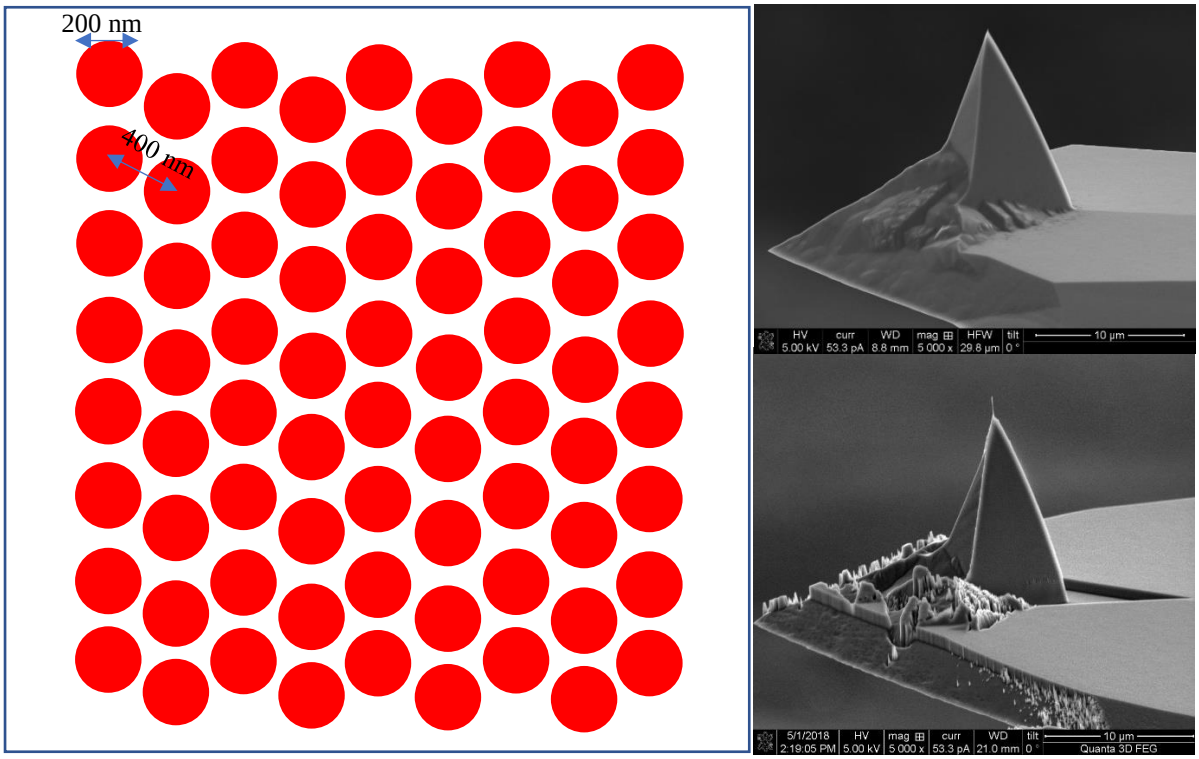

Figure 3.7 Left: Schematic of pillar array sample. Upper right: SEM image of original tip. Lower right: SEM image of our HAR tip.

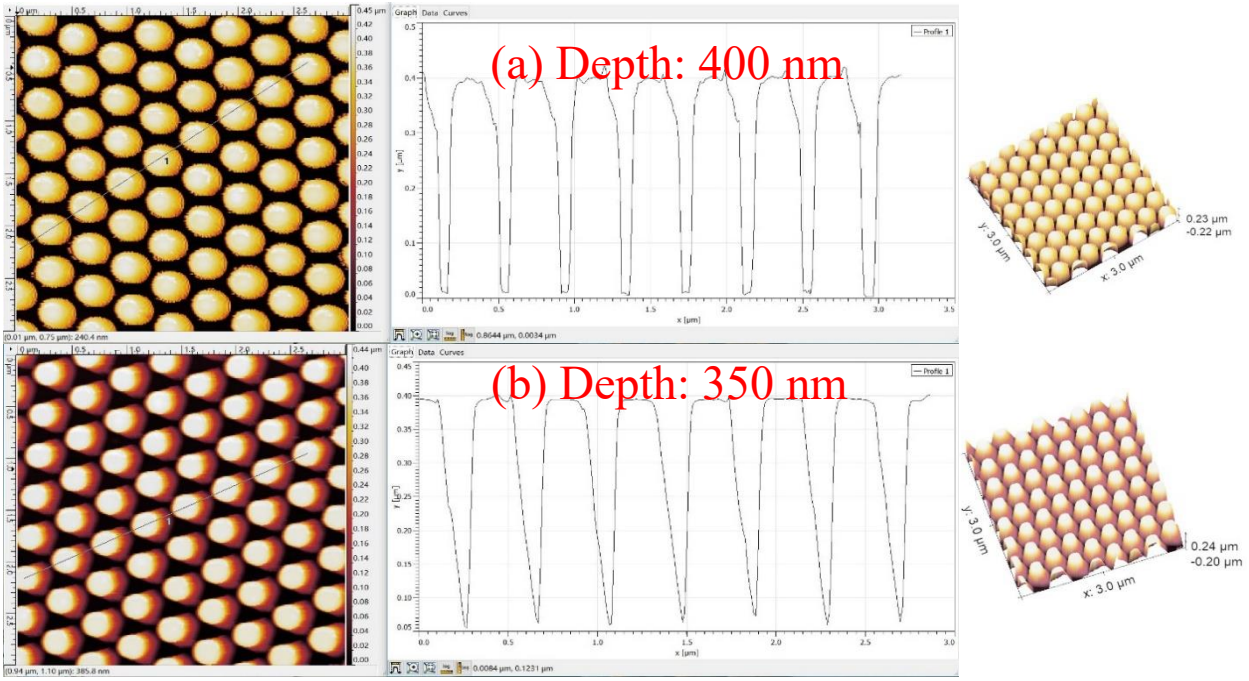

Figure 3.8 Screenshot of AFM scan result of our pillar array sample. (a) Result by using fabricated HAR tip. It can reach the sample bottom. (b) Result by using the regular commercial tip. It cannot reach the bottom.

Both commercial tip and our HAR tip were tested by a Vecco-AFM tool under tapping mode. The SEM images of both tips are shown in Fig. 3.7. Height, width, and length of cantilevers were similar. From Fig. 3.8, it is clear that our HAR tip shows a much better scan profile and higher vertical resolution than the regular commercial tip.

Also, in order to ensure that our tips can survive enough number of scanning, we scanned this sample for seven times and compared gap depth obtained from AFM result. From Fig. 3.9, after 7 scans, the depth reading didn't show a significant drop, which means our tip retained its performance even at the end of the 7^{th} scan.

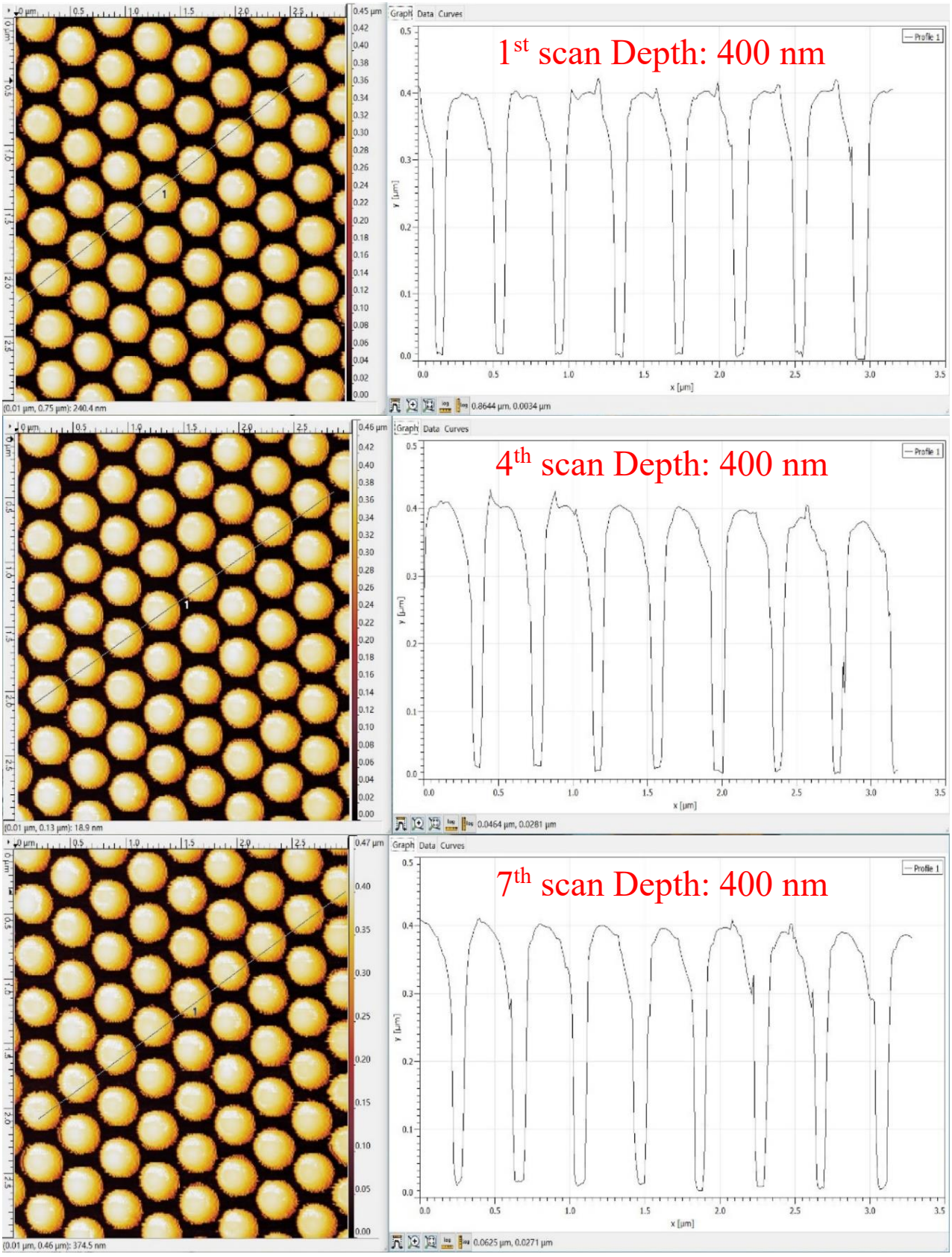

Figure 3.9 AFM scanning result of 1st, 4th, 7th scan on the same sample with the same condition of AFM scanning.

3.4 Conclusion

We have successfully developed a method to fabricate the high aspect ratio AFM probes, in batch. The main idea is to form a small Cr_2O_3 dot on the apex of each tip. This method has been applied to regular commercial tips and we successfully obtained tips with the aspect ratio up to 15:1. Later on, the performance of fabricated HAR tips was tested. Our HAR tips show a significantly better image quality compared to regular commercial tips while scanning very dense high pillar array sample. Since this method is a batch and lithography-free process, much lower cost and much higher throughput can be achieved.

Chapter 4. Batch fabrication of edge tips

This chapter presents in detail a method to obtain edge tips using nanofabrication techniques.

4.1 Background

In the previous chapter, we made high aspect ratio tips since advanced research requires a high aspect ratio tip to characterize the deep trenches or steep walls. In words, the selection of the tip is purpose-directed and dependent on specific applications.[1] Here we made a kind of probe shown in Fig. 4.1b. The tip is accurately located at the very end of the cantilever.

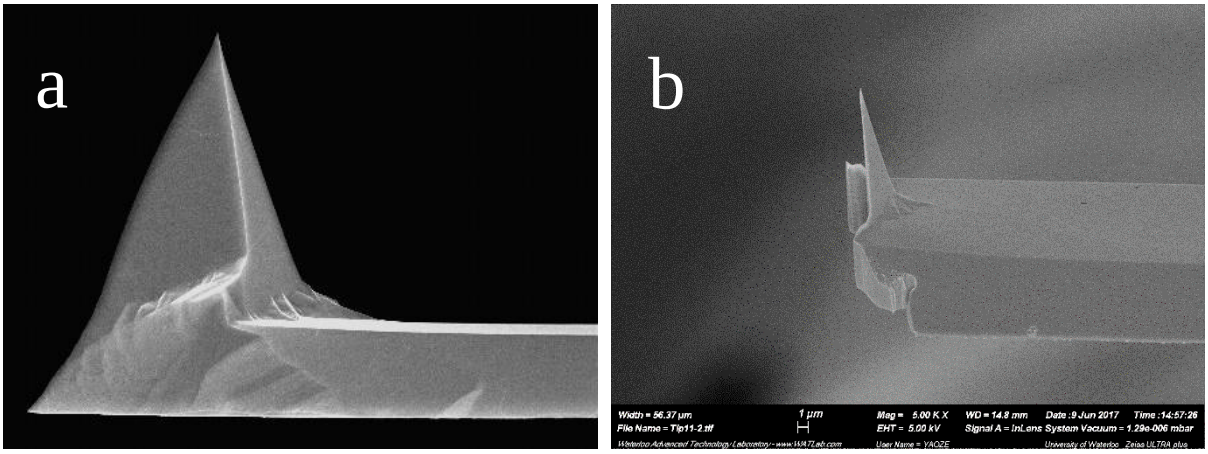

Figure 4.1 SEM images of (a) the original tip (ACT tip from Applied NanoStructures, Inc). (b) The edge tip we fabricated out of this tip.

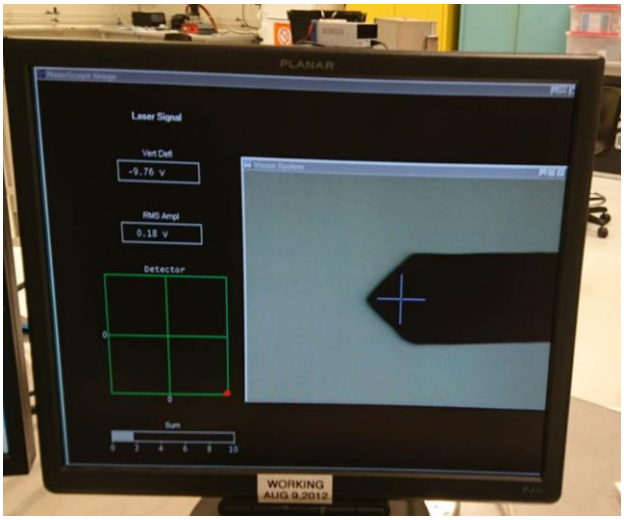

Figure 4.2 A photo of probe captured by the built-in camera in a Vecco AFM equipment. The tip location cannot be seen since the tip is viewed from the backside of the cantilever.

For regular tips, it is impossible to know accurately the tip position since the camera in AFM only captures the backside of the cantilever (Fig. 4.2). This uncertainty will result in several problems. Firstly, the scanning area must be big enough to ensure the desired areas are covered. Secondly, multiple attempts are required before finally selecting the area of interest. Both will dramatically increase the risk of damaging the sample, especially in contact mode or in a soft sample.[2] Thus, being able to directly see the tip location is the best way to solve this problem. As such, an edge probe with the tip located at the end of the cantilever is required.

4.2 Fabrication process to make edge tips

The main idea of our method is simple and straightforward: cover and protect part of the tip pyramid with masking material, modify the shape by etching away the uncovered part, remove the masking material and then do a sharpening process. So, there are four main steps: deposition of masking material, dry etch to remove unwanted part, wet etch to remove remained mask, and thermal oxidation.

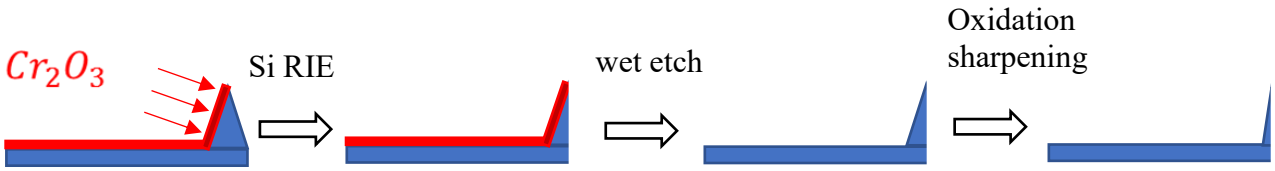

Figure 4.3 A schematic diagram of the fabrication process to make edge tip.

4.2.1 E-beam evaporation to deposit mask material

In this case, Cr_2O_3 is chosen as the masking material, and like what we did in the previous chapter, angled deposition is implemented. As we demonstrated previously, the smaller deposition angle, the more risk of Cr_2O_3 covering the other side. Because we don't want Cr_2O_3 coated on free ending side, no matter how little amount of mask, a safe larger deposition angle (60°) is selected here. After choosing the masking material and deposition angle, the next parameter is the mask layer thickness. Because the mask layer is only used for protecting underlayer, we don't need to make an exact value of thickness, as long as it is thick enough. In practice, we choose 200 nm.

4.2.2 Reactive ion etching of chromium oxide

Again, we require a selective anisotropic etching, so wet etching is excluded. We still choose a non-switching RIE recipe, instead of standard Bosch process, in order to obtain a smooth side-surface. In this case, the recipe "Temp Reza 2" (developed by Dr. Reza, University of Waterloo) employs a combination of C_4F_8 and SF_6, and the gas flow ratio is 38:22. Once the etch recipe was determined, we had to estimate etching time. Usually the AFM tip is at least 8 μm high and the etching rate for Si is around 400 nm/min, so we set the etching duration at 20 minutes. Since the selectivity between Si and Cr_2O_3 is more than 100, only 80 nm Cr_2O_3 will be consumed in Si RIE, thus some mask material will remain until the end of etching.

4.2.3 Wet etching of chromium oxide

Si RIE "cut" half of the pyramid of the tip, and then the goal of this step is to remove all the remaining masking material. Wet etch, which is isotropic and has high selectivity, is our first choice. As said before, Cr_2O_3 has similar properties to Cr both in dry and wet etch, therefore, Cr etchant can be applied to etch Cr_2O_3 as well without any modification in the recipe. The most popular recipe is a mixture of ceric ammonium nitrate, acetic acid, and water, which has the etching rate of 240 ± 20 nm/min at 45 ℃. We heated the etchant to 45 ℃ and put all the tips in it for 10 min. The sample was over etched since Cr_2O_3 layer will be much thinner after Si RIE. However, it will not attack tips (made with Si) because of the high selectivity of a chemical wet etching.

4.2.3 Thermal oxidation sharpening

Thermal oxidation is the most widely used method to sharpen the tip. It is based on different oxidation rate on different parts. The smaller the curvature, the more stress, and the lower rate. Therefore, for a cone or pyramid shape like AFM tip, the bottom part of the tip will have a much faster oxide growth rate than that of apex part; and followed by the HF etch to etch oxides, the tip will get sharpened. (shown in Fig. 4.4a)

We employed a low-cost furnace (shown in Fig. 4.4b) to do the thermal oxidation in an atmospheric environment rather than in vacuum. Tips are mounted in the high-temperature furnace chamber and we performed the oxidation process at 950 ℃ for 1 hour, and the chamber was naturally cooled down to room temperature at the end. After that, the oxide layer was stripped by using HF (1:20 diluted) for 15 minutes.

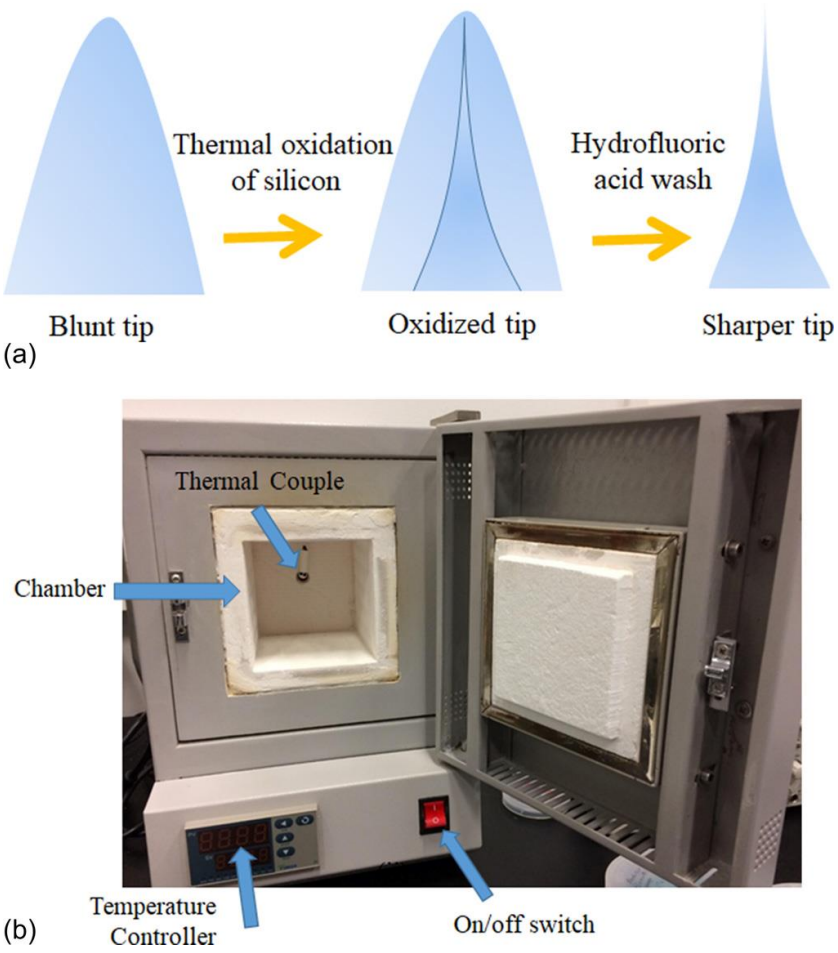

Figure 4.4 (a) Schematic drawing of oxidation sharpening process. (b) Photo of the muffle furnace used to grow oxide. The chamber size is10×10×12 cm, and it is heated by resistive heating to a maximum temperature of 1200 ℃. The heating up rate can be accurately controlled within a range of 0–15 ℃/min, but there is no active control of the cooling down rate.[3]

4.3 Results and discussion

We developed the fabrication process to make edge tips in batch. Here are some results we obtained. Fig. 4.5 presents SEM images of our tips. All of these tips are located at the end of the cantilever and have a very sharp profile. The radius of curvature on the apex is less than 10 nm when viewed from the side. However, when viewed along cantilever axis, obviously the dimension doesn't change and is still very large. (Fig. 4.6)

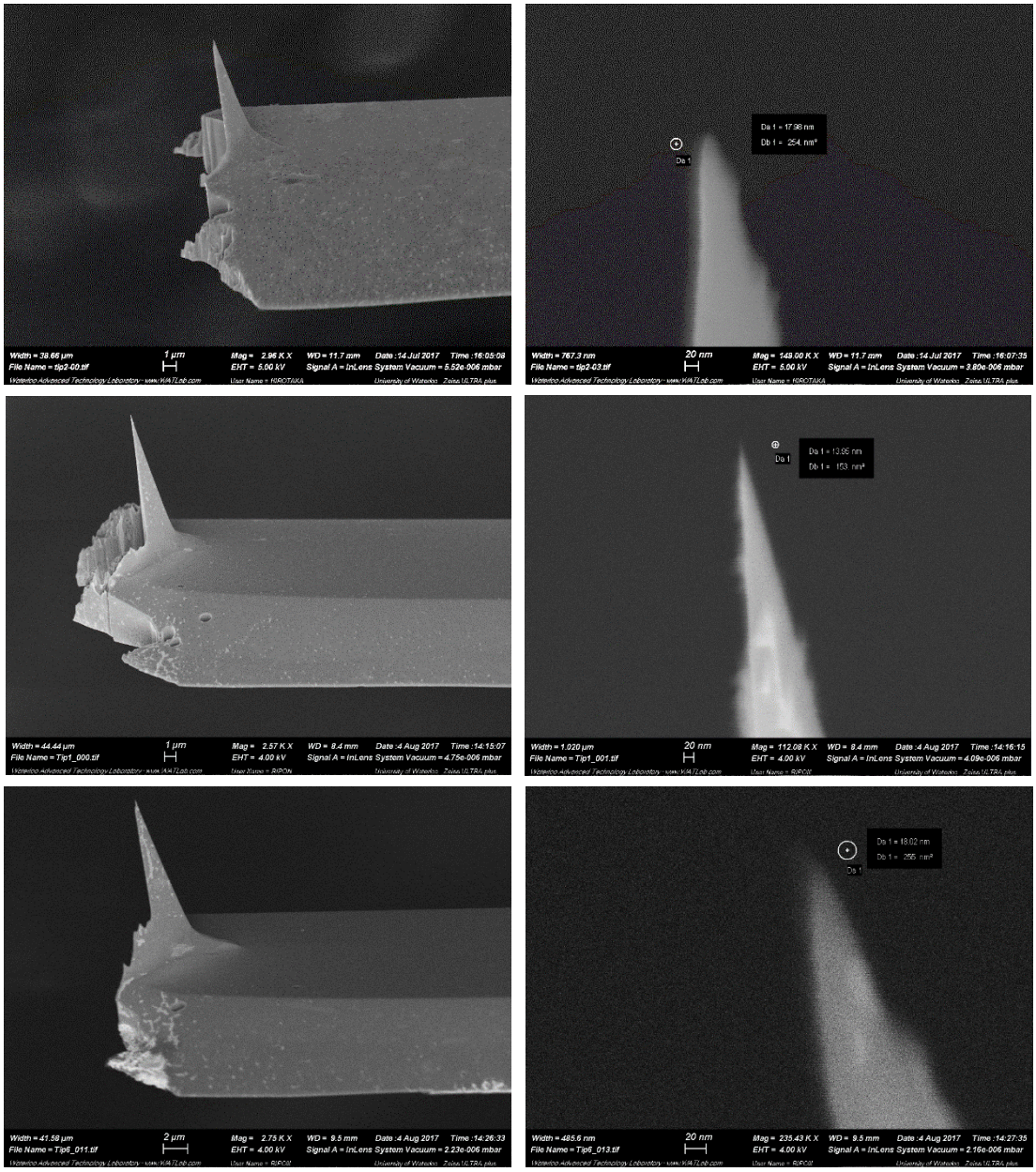

Figure 4.5 SEM images of some edge tips we fabricated.

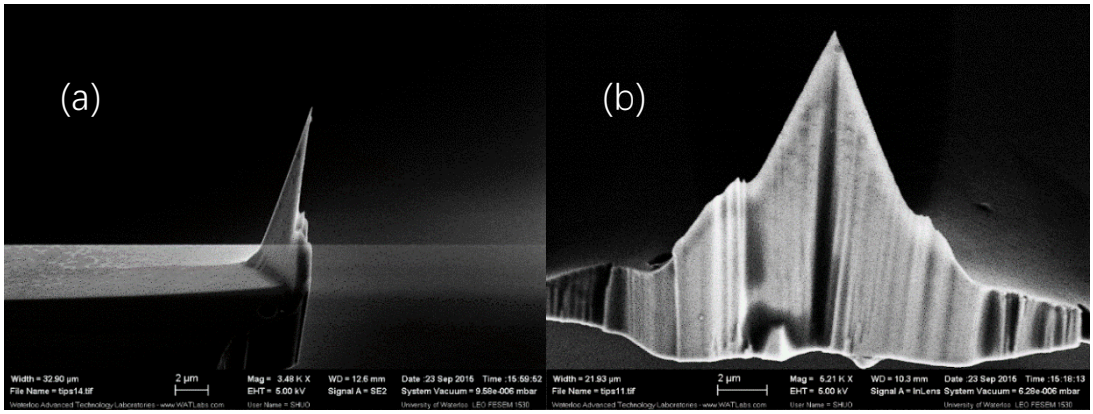

Figure 4.6 The SEM images of the same tip captured from (a) lateral side, and (b) backside. It is clearly seen that the dimension decreases significantly in one direction but remains the same in the other direction.[1]

Also, we mounted these tips in AFM to check by using the built-in camera in AFM. The main feature of tips we fabricated is that we can see the tip position by our eyes. From Fig. 4.8 we can clearly locate the tip below the cantilever, which is at the very end of the cantilever.

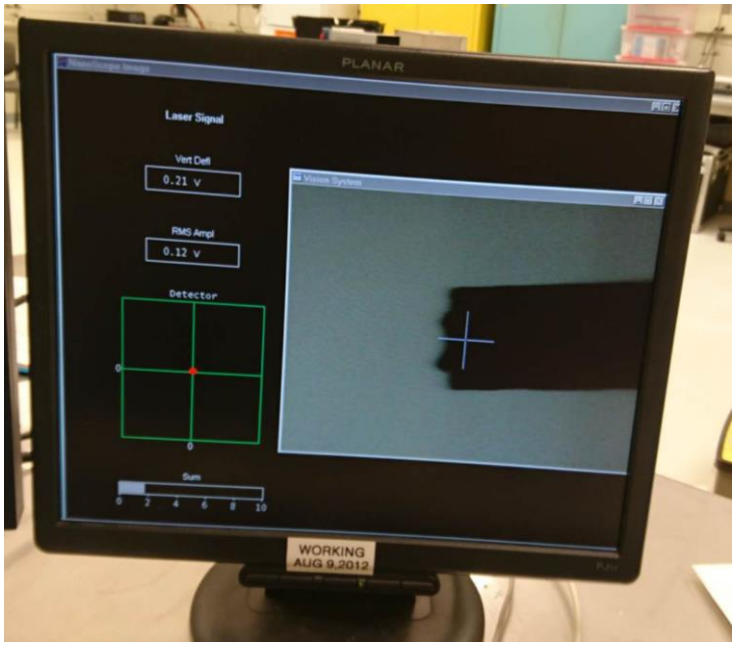

Figure 4.7 A photo captured from AFM tip calibration window. Tip position can be easily identified (at the end of the cantilever).

4.4 Conclusion

We have presented a simple and low-cost method to batch fabricate edge probes. This method has been applied to regular commercial probes and very sharp tips could be obtained followed by the thermal oxidation sharpening process. The test in AFM shows a clear location of the probe.

References

Chapter 1

[1] C. Toumey, "Why not zwergo-technology?," *Nature Nanotechnology*, vol. 6, p. 393, 07/06/online 2011.

[2] R. Saini, S. Saini, and S. Sharma, "Nanotechnology: The Future Medicine," *Journal of Cutaneous and Aesthetic Surgery*, vol. 3, pp. 32-33, Jan-Apr 2010.

[3] S. Panneerselvam and S. Choi, "Nanoinformatics: Emerging Databases and Available Tools," *International Journal of Molecular Sciences*, vol. 15, p. 7158, 2014.

[4] B. D. Gates, Q. Xu, M. Stewart, D. Ryan, C. G. Willson, and G. M. Whitesides, "New Approaches to Nanofabrication: Molding, Printing, and Other Techniques," *Chemical Reviews*, vol. 105, pp. 1171-1196, 2005/04/01 2005.

[5] M. J. Madou, "Fundamentals of microfabrication: the science of miniaturization. 2002," *ISBN-10*, vol. 1208775268.

[6] M. A. Mohammad, T. Fito, J. Chen, S. Buswell, M. Aktary, S. K. Dew, *et al.*, "The interdependence of exposure and development conditions when optimizing low-energy ebl for nano-scale resolution," in *Lithography*, ed: InTech, 2010.

[7] G. Binnig, C. F. Quate, and C. Gerber, "Atomic force microscope," *Phys Rev Lett*, vol. 56, pp. 930-933, Mar 3 1986.

[8] W. Knoll and R. C. Advincula, *Functional Polymer Films, 2 Volume Set*: John Wiley & Sons, 2013.

[9] G. W. Neudeck and R. F. Pierret, "Introduction to microelectronic fabrication," *Modular Series on Solid State Devices*, vol. 5, 2002.

Chapter 2

[1] G. Binnig, C. F. Quate, and C. Gerber, "Atomic force microscope," *Phys Rev Lett*, vol. 56, pp. 930-933, Mar 3 1986.

[2] F. J. Giessibl, "Advances in atomic force microscopy," *Reviews of modern physics*, vol. 75, p. 949, 2003.

[3] S. Tien, Q. Zou, and S. Devasia, "Iterative control of dynamics-coupling-caused errors in piezoscanners during high-speed AFM operation," *IEEE Transactions on Control Systems Technology,* vol. 13, pp. 921-931, 2005.

[4] Q. Zhong, D. Inniss, K. Kjoller, and V. Elings, "Fractured polymer/silica fiber surface studied by tapping mode atomic force microscopy," *Surface Science Letters,* vol. 290, pp. L688-L692, 1993.

[5] D. Rugar and P. Hansma, "Atomic force microscopy," *Physics today,* vol. 43, pp. 23-30, 1990.

[6] I. Y. Sokolov, G. Henderson, and F. Wicks, "The contrast mechanism for true atomic resolution by AFM in non-contact mode: quasi-non-contact mode?," *Surface science,* vol. 381, pp. L558-L562, 1997.

[7] L. Gross, F. Mohn, N. Moll, P. Liljeroth, and G. Meyer, "The chemical structure of a molecule resolved by atomic force microscopy," *Science,* vol. 325, pp. 1110-1114, 2009.

[8] N. Oyabu, O. Custance, I. Yi, Y. Sugawara, and S. Morita, "Mechanical vertical manipulation of selected single atoms by soft nanoindentation using near contact atomic force microscopy," *Physical Review Letters,* vol. 90, p. 176102, 2003.

[9] O. Custance, R. Perez, and S. Morita, "Atomic force microscopy as a tool for atom manipulation," *Nature nanotechnology,* vol. 4, p. 803, 2009.

[10] R. D. Piner, J. Zhu, F. Xu, S. Hong, and C. A. Mirkin, "" Dip-pen" nanolithography," *science,* vol. 283, pp. 661-663, 1999.

[11] D. Wang, L. Tsau, and K. Wang, "Nanometer-structure writing on Si (100) surfaces using a non-contact-mode atomic force microscope," *Applied physics letters,* vol. 65, pp. 1415-1417, 1994.

[12] Z. J. Davis, G. Abadal, O. Hansen, X. Borise, N. Barniol, F. Perez-Murano, *et al.*, "AFM lithography of aluminum for fabrication of nanomechanical systems," *Ultramicroscopy,* vol. 97, pp. 467-472, 2003.

[13] P. Russell and O. Krause, "AFM Probe Manufacturing," *NanoWorld Services,* 2008.

[14] O. H. Willemsen, M. M. Snel, A. Cambi, J. Greve, B. G. De Grooth, and C. G. Figdor, "Biomolecular interactions measured by atomic force microscopy," *Biophysical journal,* vol. 79, pp. 3267-3281, 2000.

[15] J.-d. Li, J. Xie, W. Xue, and D.-m. Wu, "Fabrication of cantilever with self-sharpening nano-silicon-tip for AFM applications," *Microsystem technologies,* vol. 19, pp. 285-290, 2013.

[16] "“AFM tip basics”- exposed by NanoWorld Services GmbH https://www.agilent.com/cs/library/slidepresentation/Public/AFM%20Probe%20ManufacturingNanoworld_tip_technologyPRussell07.pdf."

[17] G. Villanueva, J. Plaza, A. Sanchez, K. Zinoviev, F. Perez-Murano, and J. Bausells, "DRIE based novel technique for AFM probes fabrication," *Microelectronic engineering,* vol. 84, pp. 1132-1135, 2007.

[18] R. Marcus, T. Ravi, T. Gmitter, K. Chin, D. Liu, W. Orvis, *et al.*, "Formation of silicon tips with< 1 nm radius," *Applied Physics Letters,* vol. 56, pp. 236-238, 1990.

[19] A. Folch, M. S. Wrighton, and M. A. Schmidt, "Microfabrication of oxidation-sharpened silicon tips on silicon nitride cantilevers for atomic force microscopy," *Journal of microelectromechanical systems,* vol. 6, pp. 303-306, 1997.

[20] M. A. R. Alves, D. Takeuti, and E. Braga, "Fabrication of sharp silicon tips employing anisotropic wet etching and reactive ion etching," *Microelectronics Journal,* vol. 36, pp. 51-54, 2005.

[21] K. Westra, A. Mitchell, and D. Thomson, "Tip artifacts in atomic force microscope imaging of thin film surfaces," *Journal of Applied Physics,* vol. 74, pp. 3608-3610, 1993.

[22] Y. Fu, W. Zhou, L. E. Lim, C. Du, X. Luo, X. Dong, *et al.*, "Geometrical characterization issues of plasmonic nanostructures with depth-tuned grooves for beam shaping," *Optical Engineering,* vol. 45, p. 108001, 2006.

[23] R. A. Oliver, "Advances in AFM for the electrical characterization of semiconductors," *Reports on Progress in Physics,* vol. 71, p. 076501, 2008.

[24] A. Noy, D. V. Vezenov, and C. M. Lieber, "Chemical force microscopy," *Annual Review of Materials Science,* vol. 27, pp. 381-421, 1997.

[25] J. Brown, P. Kocher, C. S. Ramanujan, D. N. Sharp, K. Torimitsu, and J. F. Ryan, "Electrically conducting, ultra-sharp, high aspect-ratio probes for AFM fabricated by electron-beam-induced deposition of platinum," *Ultramicroscopy,* vol. 133, pp. 62-66, 2013.

[26] I. Rangelow, "Sharp silicon tips for AFM and field emission," *Microelectronic Engineering,* vol. 23, pp. 369-372, 1994.

[27] Y. Shingaya, T. Nakayama, and M. Aono, "Carbon nanotube tip for scanning tunneling microscopy," *Physica B: Condensed Matter,* vol. 323, pp. 153-155, 2002.

[28] H. Dai, J. H. Hafner, A. G. Rinzler, D. T. Colbert, and R. E. Smalley, "Nanotubes as nanoprobes in scanning probe microscopy," *Nature,* vol. 384, p. 147, 1996.

[29] N. R. Wilson and J. V. Macpherson, "Carbon nanotube tips for atomic force microscopy," *Nature nanotechnology,* vol. 4, p. 483, 2009.

[30] J. H. Hafner, C. L. Cheung, and C. M. Lieber, "Growth of nanotubes for probe microscopy tips," *Nature,* vol. 398, pp. 761-762, 04/29/print 1999.

Chapter 3

[1] G. Guisbiers, S. Strehle, and M. Wautelet, "Modeling of residual stresses in thin films deposited by electron beam evaporation," *Microelectronic Engineering,* vol. 82, pp. 665-669, 2005.

[2] S. Zheng, "Nanofabrication of direct positioning atomic force microscope (AFM) probes and a novel method to attain controllable lift-off," University of Waterloo, 2017.

[3] C. Chang, Y.-F. Wang, Y. Kanamori, J.-J. Shih, Y. Kawai, C.-K. Lee, *et al.*, "Etching submicrometer trenches by using the Bosch process and its application to the fabrication of antireflection structures," *Journal of micromechanics and microengineering,* vol. 15, p. 580, 2005.

Chapter 4

[1] S. Zheng, "Nanofabrication of direct positioning atomic force microscope (AFM) probes and a novel method to attain controllable lift-off," University of Waterloo, 2017.

[2] S. Zheng, C. Zhu, R. K. Dey, and B. Cui, "Batch fabrication of AFM probes with direct positioning capability," *Journal of Vacuum Science & Technology B, Nanotechnology and Microelectronics: Materials, Processing, Measurement, and Phenomena,* vol. 35, p. 06GC02, 2017.

[3] R. K. Dey, J. Shen, and B. Cui, "Oxidation sharpening of silicon tips in the atmospheric environment," *Journal of Vacuum Science & Technology B, Nanotechnology and Microelectronics: Materials, Processing, Measurement, and Phenomena,* vol. 35, p. 06GC01, 2017.